SULPHUR DIOXIDE CAPTURE UNDER FLUIDIZED BED COMBUSTION CONDITIONS

Tholakele Prisca Ngeleka

B. Tech. (Mangosuthu Technikon - Durban)

This dissertation is presented in partial fulfillment of the requirements for the degree Master of Science (Engineering Science) in the School of Chemical and Minerals Engineering at North-West University, Potchefstroom Campus.

Supervisor: Professor R.C. Everson

Co-supervisor: Professor H.W.J.P. Neomagus

DECLARATION

Hereby I, Tholakele Prisca Ngeleka, declare that the dissertation with the title SULPHUR DIOXIDE CAPTURE UNDER FLUIDIZED BED COMBUSTION CONDITIONS in partial fulfilment of the requirements for the degree Master of Science (Engineering Science), is my work and has not been submitted at any other university either in whole or in part.

Signed at Potchefstroom on the ...16th.....day of ...March.....2005.

.....TPNgeleka.....

T.P. Ngeleka

ACKNOWLEGDEMENTS

I would like to express my sincere gratitude to people who have assisted me in various ways throughout my research.

Above all, God Almighty, thank you for giving me the wonderful opportunities and people to work with. For the strength and grace you blessed my way every day of my life.

Department of Chemical and Minerals Engineering at the North West University for believing in me and give me the opportunity to conduct this research.

Professor R.C. Everson and Professor H.W.J.P. Neomagus for helping me with my studies right from the beginning.

Mr Rufaro Kaitano for the support throughout the study.

Mr Henry van Zyl, Mr Jan Kroeze and Mr Adrian Brock for the construction and upkeep of the experimental apparatus.

Eskom (TESP) for their financial support

Parents and friends for encouragements love support, and lot of prayers.

ABSTRACT

An investigation was undertaken to determine the desulphurization properties of industrially available dolomites for use in fluidized bed (coal) combustion (FBC). The performance and kinetics of sulphur dioxide capture were examined at atmospheric pressure under conditions favouring the presence of calcium oxide. Experimentation was carried out with a thermo gravimetric analyzer with typical gas mixtures occurring in FBC consisting of 2500ppm sulphur dioxide and carbon dioxide concentrations varying between 8% and 25% (mole). The structural properties that are important in desulphurization reactions were determined by BET and mercury porosimetry methods and it was found that the dolomite samples consisted of a non-uniform distribution of pore sizes with porosities (±25%) similar to dolomites used by other investigators. Experimentation consisted of calcination with pure nitrogen of the raw dolomite samples, followed by reaction with different gas mixtures to assess possible recarbonation (phase transition of calcium oxide) accompanying sulphation. It was found that phase transition temperatures and carbon dioxide partial pressures for the relevant calcium - based compounds were different to predictions from thermodynamic equilibrium calculations involving pure compounds. This effect is attributed to the presence of these compounds in a mineral complex structure and the impurities present, which was also observed by other investigators. Both calcium oxide and calcium carbonate are suitable for desulphurization and in this study attention was confined essentially to the calcium oxide phase. Sulphation with calcium oxide was found to occur above 850°C with low carbon dioxide concentrations, and results were obtained which did not show any blocking of pores as a result of molar density differences. Calcium oxide conversions of the order of 10% to 15% were obtained after 120 minutes (on-line), which compared well with some results in the literature. A shrinking core model incorporating an effective diffusion coefficient accounting for the structural changes was found to be valid for most experiments.

TABLE OF CONTENTS

LIST OF FIGURES

LIST OF TABLES

NOMENCLATURE

A, B, C, D	constants	(-)
C_g	bulk gas concentration of SO_2	(mol/m^3)
C_p	specific heat capacity	(kJ/ kg K)
D	diffusion coefficient, diffusivity	(m^2/s)
E_a	activation energy	(J/mol)
G^o	standard Gibbs Free energy	(J/mol)
H_0^o	standard heat of reaction at reference temperature	(J/mol)
K	equilibrium constant	(bar)
k_s	reaction rate constant	(m/s)
Mm	molar mass	(kg/kmol)
M_o	sample mass after calcination	(mg)
p	partial pressure	(bar)
R_{p_a}	*adsorbent particle radius*	(μm)
$(\overline{r_p})$	average pore radius	(μm)
R	universal gas constant	(J/mol K)
T	temperature	(°C and K)
T_0	*reference temperature*	(°C and K)
t	time	(min)
V	volume	(m^3)
X	overall conversion	(-)
x_{CaO}	mass fraction CaO in solid	(wt%)
Z	molar volume ratio solid reactant/product	(-)

Greek letters

ε	particle porosity	(-)
ε_0	initial particle porosity	(-)
ρ_{mol}	molar density of solid	(mol/m^3)
ρ_{p_a}	initial adsorbent particle density	(kg/m^3)

τ	tortuosity	(-)
τ_D	time scale diffusion	(-)
τ_R	time scale reaction	(-)
τ_0	temperature ratio	(-)
ϕ	Thiele modulus	(-)

Subscripts

D	diffusion
eff	effective
g	gas
k	Knudsen
m	molecular
o	standard
p	pore
p_a	particle
pl	product layer
R	reaction
s	solid
T	molecular +knudsen
u	unreacted

Superscripts

o	reference

Abbreviations

BFBC	bubbling fluidized bed combustion
CFBC	circulating fluidized bed combustion
FBC	fluidized bed combustion
LRR	laboratory recycle reactor
PFBC	pressurized fluidized bed combustion
SEM	scanning electron microscope
TGA	thermo gravimetric analyzer

USC	unreacted shrinking core model
USC - VED	unreacted shrinking core model with variable effective diffusivity

CHAPTER 1
INTRODUCTION

1.1 General

Coal has traditionally dominated the energy supply sector in South Africa and its use worldwide is also expected to increase. South Africa is the fifth largest coal producer in the world and accounts for an average of 224 million tonnes of marketable coal annually (Eskom, 2003). Twenty five percent of the coal produced is exported and the remainder of South Africa's coal production (including discards) is used in the industrial, government and domestic sectors. The major coal consumers in South Africa are the electricity generation company Eskom and the coal – to - liquid fuels/chemicals company Sasol (Eskom, 2003).

One major problem is that the coal presently used in South Africa especially in the future is of poor quality and the major environmental problem is the production of pollutant flue gases during coal combustion and gasification. The coal reserves in South Africa have a low heating value coal, high content of sulphur - containing minerals (2 wt % sulphur) and a high content of ash (up to 45 wt %) (Van der Riet, 2005).

Environmental concerns pose the main challenge to coal as a source of energy. Not only does the burning of coal cause pollution, the mining activities to extract the coal also have a severe impact on the environment. Flue gases from coal combustion pollute the atmosphere and the associated ashes pollute the soil and water. The chief pollutants are nitrogen oxides and sulphur oxides, particulate emission, and green house gases such as carbon dioxide (CO_2), methane (CH_4) and water vapor. The sulphur oxides (SO_x) emissions from combustion systems have a significant impact on the environment as it causes acid rain, which could damage the ecosystem and human health (Irfan and Balci, 2002). Another negative effect of coal utilization is the formation of photochemical smog as a result of formation of nitrogen - based oxides (NO_x) especially at high temperature.

However, the implementation of measures to control the emission of sulphur dioxide (SO_2) is of vital importance. There are several options for accomplishing the clean coal combustion such as integrated gasification combined cycle (IGCC), and fluidized bed combustion (FBC) technologies that are particularly attractive because of their flexibility and the associated environmental benefits (Chen *et al.*, 2001, Topper *et al.*, 1994 and Partanen, 2004). FBC is an efficient technology for the variety of fuels and the reduction of SO_2 emissions as it allows the emission control during combustion (Partanen, 2004, and Zhangfa, 2003). Emission control inside the fluidized bed, by injecting adsorbents such as limestone and dolomite in the combustors is also advantageous from the perspective of cost (Partanen, 2004).

1.2 Motivation

Eskom relies on coal - fired power plants to produce approximately 90 % of South Africa's electricity, using a relatively poor quality coal with high sulphur and ash content as mentioned above. Eskom in conjunction with the Centre for Coal Studies at the North - West University (Potchefstroom campus), has identified a need for research concerning the reaction between sulphur dioxide and different dolomites as used in their FBC pilot plant. The addition of limestone and dolomite to the bed is a widely used method of controlling SO_2 emissions in the coal fired plants and fluidised bed combustion of fuels containing sulphur compounds. Various calcium-based systems for SO_2 removal are described in the literature (Yrjas *et al.*, 1995, Zevenhoven *et al.*, 1996, 1998, Mattisson and Lyngfelt, 1998, Alvarez and Gonzalez, 1999, Wang *et al.*, 2002, Zhang *et al.*, 2003, Adanez *et. al.*, 2004, and Mahesh *et al.*, 2004), the focus being the effectiveness of SO_2 removal.

Fluidized bed combustion (FBC) can be carried out at atmospheric pressure and at higher pressures at temperatures within the range 750°C to 950°C and with concentrations of carbon dioxide, which vary significantly within the fluidized bed. This has a marked effect on the state of adsorbent present for sulphation (CaO or $CaCO_3$) and needs to be considered during the design stages of fluidized bed combustors.

Many studies have been confined to high pressure (Tullin and Ljungstrom, 1989, Iisa and Hupa, 1990, Iisa, 1992, Fernouli and Lynn, 1995, Fuertes *et al.*, 1995, Zevenhoven *et al.*, 1996,1998a and 1998b, Tadaaki *et al.*, 2002, Trikkel and Kuusik, 2003), and high concentrations of carbon dioxide involving the sulphation of $CaCO_3$ while sulphation at atmospheric pressure with low concentrations of carbon dioxide and at temperatures larger than 850°C, involving CaO, has not received as much attention. It should be noted that CaO is rather unstable (phase instability) at elevated temperature as a result of sintering (Bogwardt *et al.*, 1986).

1.3 Objectives of the study

An investigation was undertaken to determine the desulphurizing properties of typical industrial-type dolomites used in fluidized bed coal combustion (FBC) operating at atmospheric pressure with specific attention to the capture of sulphur dioxide with calcium oxide. For this purpose the following was carried out:

- The determination of the temperature and carbon dioxide concentration ranges at which desulphurization with calcium oxide or calcium carbonate occurs.
- The determination of the adsorption performance of the dolomites under conditions favouring sulphation of calcium oxide only.
- The evaluation of a suitable reaction rate model for the sulphation of calcium oxide only based on the physical characteristics of the dolomites.

1.4 Scope of this dissertation.

In this study, the sulphur dioxide capture using industrial type dolomites from a typical FBC mixture consisting of 2500 ppm SO_2 with CO_2, O_2 and N_2 was investigated. The physical properties of dolomites were determined using BET, mercury porosimetry and scanning electron microscope measurements, and reactivity determinations performed using a thermo gravimetric analyzer. Results were obtained which show the characteristics and the reactive properties of two different dolomites determined at FBC reaction conditions operating at atmospheric pressure. The well - known shrinking core model with a modification to incorporate the effect of structural changes (varying diffusivity) for prediction of the reaction was evaluated and relevant parameters determined.

An overview of the available literature, on sulphur dioxide capture by limestone and dolomite is presented in Chapter 2. The review of desulphurization in the fluidized bed combustion and the chemistry of sulphur dioxide reacting with calcium - based adsorbents are discussed. Adsorbents for sulphur dioxide capture are reviewed with respect to structural properties, advantages and disadvantages, the availability was also considered. Reaction kinetics for desulphurization and different models that have been used by different researchers are reviewed. An overview of the experimental apparatus is also provided.

A derivation of the model evaluated with a description and assumptions is given in Chapter 3. A description of the experimental apparatus and methods used in this study is given in Chapter 4 with a detailed discussion of the high-pressure thermo gravimetric analyzer (TGA). Materials used are listed which are given in terms of their origin and structural properties where applicable.

Chapter 5 presents the physical properties of the dolomites and the reaction results conducted with the TGA as well as the results from the modelling. The results of this study are also compared with the results obtained by other researchers.

Finally in Chapter 6 conclusions from the results are drawn and recommendations are made based on the findings of the study.

CHAPTER 2
LITERATURE SURVEY

2.1 Introduction

This chapter presents a relevant literature review of FBC and of SO_2 capture with calcium - based adsorbents as a means of coal combustion emissions control. Section 2.2 presents an overview of desulphurization in FBC with an account of materials used (adsorbents) in Section 2.3. Chemical and physical characteristics of adsorbents used by other researchers are reviewed together with the chemical reactions. Section 2.4 summarizes the desulphurization kinetics, and gives an overview of possible models. Finally the equipment used for reactivity measurements is discussed in Section 2.5.

2.2 Desulphurization in fluidized bed combustion

The use of low ranked coal worldwide (poor quality) has been challenging for the design and construction of coal fired power plants. With poor quality coal, which contain lot of sulphur compounds, and with the ever more stringent environmental legislation, advanced technologies are required. There is a shift from pulverized coal combustion to fluidized bed combustion and it is clear from the open literature that fluidized bed combustion technology is a more efficient, economically and environmentally sound combustion process for a wide variety of fuels (Partanen, 2004). Fluidized bed combustion technologies include atmospheric pressure fluidized bed combustion (APFBC) and pressurized fluidized bed combustion (PFBC) utilising both bubbling fluidized bed combustion (BFBC) and circulating fluidized bed combustion (CFBC). Flue gas emissions in fluidized bed combustion can be controlled by injecting adsorbents such as limestone and dolomite into the bed, and the subsequent removal of ash together with reacted adsorbent (Zhangfa, 2003, Partanen, 2004).

When calcium based adsorbents (limestone and dolomite) are injected into the furnace of APFBC, they decompose to give calcium oxide (CaO) (Zhangfa, 2003) assuming perfect mixture, which reacts with SO_2 in the presence of oxygen to form a solid product calcium sulphate ($CaSO_4$).

In PFBC, calcium carbonate does not decompose owing to the high partial pressure of carbon dioxide (CO_2), and SO_2 is captured directly by $CaCO_3$.

Studies on industrial fluidized bed combustion desulphurization, have been conducted by many investigators, and only some are listed in Table 2.1 which include the publications of Fernadez and Lyngfelt, (2001), Stencel *et al.*, (1995) Tadaaki *et al.*, (2002) Hao and Bernard, (1998) and Wasi and Bernard, (1995). The details of the experiments are given in this table, which can be seen to be quite different. This table shows the different conditions used operating with different adsorbent together with different coals.

2.3 Adsorbents for sulphur dioxide capture

2.3.1 Materials

Calcium based adsorbents such as Limestone ($CaCO_3$), dolomite ($CaMg(CO_3)_2$), and lime (CaO) are widely used. Calcium acetate synthesized from natural limestone has also been used in situ for removal of sulphur (Zhang *et al.*, 2003). Another solid used for the removal of SO_2 in the fluidized bed combustion is sodium carbonate (Na_2CO_3) (Wang *et al.*, 2002). Due to availability and low costs, limestone and dolomite have been most widely used for SO_2 capture in industrial power plants and have been examined in detail by many researchers (Alvarez and Gonzalez, 1999, Zevenhoven *et al.*,1998 (a) and (b), Yrjas *et al.*,1995, Irfan and Balci, 2002, Garcia *et al.*, 2002, Tsutomu *et al.*, 2003).

2.3.2 Composition and physical characteristics

The chemical composition and structural properties of calcium based adsorbents used in the flue gas desulphurization are of vital importance for the determination of mechanisms involved in the calcination and sulphation processes taking place in fluidized bed combustion. The presence of impurities such as iron oxides and magnesium compounds can have an effect on the structural changes (Alvarez and Gonzalez, 1999). They have reported that Fe oxides seem to catalyse sulphation and the inert MgO in the adsorbent gives a more porous structure.

Table 2.1: Summary of experimental fluidized bed combustors examined by other investigators.

Investigator	Utility	Capacity (MW)	Adsorbents	Temperature (°C)	Fuel
Wasi and Bernard, (1995)	FBC combustor	N/A	Limestone	850	Dawmill Bituminous coal (1.66 wt %S)
Stencel *et al.*, (1995)	Bench scale reactor	N/A	Phosphoric acid	N/A	Bituminous coal (3.24 wt % S)
Fernadez & Lyngfelt, (2001)	CFFB	12	Sand, Limestone	850	Bituminous coal (1.1 wt % S)
Tadaaki *et al.*, (2002)	PFB combustor	71	Limestone	827 - 862	B A coal (0.32 wt %S)
Nowak & Muskala, (2001)	MSFB, CFB combustors	N/A	$CaCO_3$, $Ca(OH)_2$	750 - 850	Brown hard coal
Hao & Bernard, (1998)	CFBC system	N/A	Limestone	N/A	Coal (1.26 wt % S)
Nimmo *et al.*, 2004	PF Furnace	80	Calcium magnesium acetate (CMA) (mixture of dolomitic lime and acetic acid)	1100 - 1200	Bituminous coal (1.9 % S)

Structural properties which include porosity, pore size distribution, particle size, specific surface area, and particle density are key parameters for assessing the reactivity properties of the adsorbents. These structural properties determine essentially the relative importance of diffusion (porosity) and reaction (surface area) within the adsorbents. The particle density can be measured using helium-pycnometry, the internal surface area using a BET nitrogen adsorption method, and particle porosity and pore size distribution using mercury penetration porosimetry (Adanez *et al.*, 1994, Zevenhoven *et al.*, 1998 (a), 1998 (b), Alvarez *et al.*, 1999,). Examples of limestones and dolomites examined by Yrjas *et al.*, 1995 and Zevenhoven *et al.*, 1998 (a) are given in Tables 2.2 and 2.3 which consists of the respective chemical and structural properties. Chemical composition values given in Table 2.2 showed a small difference, which resulted in insignificant difference in their reactivity. With structural properties shown in Table 2.3, Stevns chalk's specific surface area was higher compared to the other adsorbents reported and it was also observed that its reactivity was higher. Examples of other limestones and dolomites studied can be seen in the publications of Ulerich *et al.*, (1980), Irfan and Balci, (2002), and Ozer *et al.*, (2002).

Table 2.2: Chemical compositions (wt %) of adsorbents tested (Yrjas *et al.*,1995)

Absorbents	C	Si	Al	Fe	Mn	Ti	Mg	Ca	CaO	MgO
Limestones										
1 Faxe Bryozo	11.9	0.21	0.053	0.056	0.015	0.006	0.26	39.4	55.1	0.43
2 Faxe Bryozo + Fe	11.8	0.26	0.058	0.406	0.031	0.012	0.19	39.2	54.8	0.31
3 Faxe Koral	11.9	0.11	0.021	0.049	0.015	0.006	0.28	39.5	55.2	0.46
4 Faxe Koral+Fe	11.9	0.10	0.026	0.224	0.023	0.006	0.29	39.3	55.0	0.48
5 Stevns Chalk	11.9	0.17	0.037	0.028	0.008	0.006	0.17	39.5	55.2	0.29
6 Ignaberga	10.9	3.89	0.206	0.154	0.023	0.036	0.33	35.6	49.8	0.55
7 Forby	11.3	1.60	0.380	0.25	0.008	0.024	0.68	37.3	52.2	1.13
8 Carmeuse	11.0	2.46	0.704	0.182	0.008	0.024	0.61	36.3	50.8	1.01
9 Gotland	11.3	1.56	0.672	0.455	0.015	0.042	0.83	36.2	50.7	1.37
10 Iowa	11.8	0.28	<0.10	0.14			0.14	39.1	54.7	0.23
11 Japanese	12.0	0.03	0.035	0.02			0.42	38.8	54.3	0.70
Dolomites										
12 Malaga	12.9	0.04	0.048	0.035	0.00	0.012	12.9	22.1	30.9	21.4
13 Silkainen	7.17			0.11			10.5	16.6	23.2	17.4
14 Virginia	12.6			0.10			11.6	24.2	33.9	19.2
15 Sibbo	11.9	1.80	0.36	0.33	0.02		9.5	24.2	33.9	15.8
16 Myonit	9.4			0.33			7.5	19	26.5	12.4
17 Glanshammer	12.1			0.32			12.1	18.1	25.3	20.1

Table 2.3: Chemical properties of limestones and dolomites (Zevenhoven *et al.* 1998(b))

Adsorbents	$CaCO_3$[a] (wt %)	$MgCO_3$ (wt %)	$\rho_{mol,CaCO_3}$[a] (mol/m^3)	Specific surface (m^2/g)	Particle Porosity (-)	Particle density (kg/m^3)	Average pore diameter (μm)
Limestones							
Faxe Bryozo	98.4	0.90	16842	2.25	0.178	1681	0.323
Faxe Bryozo/Fe	97.9	0.65	23568	1.49	0.075	2416	0.251
Stevns Chalk	98.6	0.61	13273	4.63	0.324	1351	0.412
Ignaberga	88.9	1.15	15608	2.94	0.077	1762	0.209
Gotland	90.4	2.87	25095	3.74	0.063	2786	0.074
Dolomites							
Sibbo	60.4	32.9	16385	0.93 - 2.85	0.022-0.206	2727-2214	0.112
Wisconsin Wilbur	47.4	26.0	13484	0.060 - 0.241	0.010-0.162	2855-2416	0.291

[a]Calculated.

2.3.3 Chemistry

Equation (2.1) to (2.4) are the calcination reactions of adsorbent (Tullin and Ljungstrom, 1989, Yrjas *et al.*,1995, Wang *et al.* 2002, Cigdem *et al.*, 2001).

$$CaCO_{3(s)} = CaO_{(s)} + CO_{2(g)} \quad (2.1)$$

$$MgCa(CO_3)_{2(s)} = CaO_{(s)} + MgO_{(s)} + CO_{2(g)} \quad (2.2)$$

$$Ca(OH)_{2(s)} = CaO_{(s)} + H_2O_{(g)} \quad (2.3)$$

$$2[NaHCO_3\ Na_2CO_3\ 2H_2O]_{(s)} = 3Na_2CO_{3(s)} + CO_{2(g)} + 5H_2O_{(g)} \quad (2.4)$$

The sulphation reactions are given by equations (2.5) to (2.7). It is well known that MgO does not react with SO_2 (Zevenhoven *et al.*, 1998b)

$$CaO_{(s)} + 0.5\ O_{2(g)} + SO_{2\ (g)} = CaSO_{4(s)} \quad (2.5)$$

$$Na_2CO_{3(s)} + 0.5\ O_{2(g)} + SO_{2(g)} = Na_2SO_{4(s)} + CO_{2(g)} \quad (2.6)$$

$$CaCO_{3(s)} + 0.5O_{2(g)} + SO_{2(g)} = CaSO_{4(s)} + CO_{2(g)} \quad (2.7)$$

2.3.4 Solid phase equilibrium

The calcination of calcium and magnesium carbonate is dependant on both temperature and CO_2 partial pressure (Figure 5.9). Under atmospheric conditions the calcination process occurs according to equations (2.1 and 2.2). At high - pressure conditions, where the partial pressure of CO_2 is relatively high the calcination of $CaCO_3$ does not occur whilst $MgCO_3$ calcines even at a high pressure. A $CaCO_3$ – CaO – CO_2 phase equilibrium diagram based on fundamental thermodynamics has been published (Yrjas *et al.*, 1995, Partanen, 2004) as well as $MgCO_3$ – MgO – CO_2 diagram (Fuertes *et al.*, 1995). From these diagrams it can be seen that at 850°C and a total pressure of 1 bar, calcination of $CaCO_3$ occurs if the partial pressure of CO_2 is below 0.5 bar. Whilst at a concentration of 20% CO_2, and a total pressure of 15 bar, $CaCO_3$ does not calcine below a temperature of 970°C with a corresponding value for $MgCO_3$ being 340°C.

2.4 Reactivity of adsorbents.

Solid gas reaction kinetics of SO_2 reaction with $CaCO_3$/CaO is of great practical importance in the design and optimization of desulphurization process and many fundamental bench scale and laboratory studies, on the SO_2 reactions with limestone and dolomite have been conducted (Table 2.4). Such studies, have been performed by Dam - Johansen and Ostergaard, (1991), Fuertes *et al.*, (1995), Yrjas *et al.*, (1995), Zevenhoven *et al.*, (1998) (a) and (b), Alvarez and Gonzalez, (1999), and Wang *et al.*, (2002).

Yrjas *et al.*, (1995), studied the performance of sulphur adsorption capacities of different limestones and dolomites under both atmospheric and pressurized

combustion conditions. The results showed the SO_2 conversion rate was strongly dependent on the type of the adsorbent. At temperature of 850°C and a pressure of 1.5 MPa and a reaction time of 120 minutes, the conversion varied between 7 and 83 % for the different adsorbents. The temperature effect under pressurized combustion conditions was also studied. At higher temperature of 950°C, significantly higher conversions were obtained for most adsorbents, and were explained by an improved diffusion rate through the product layer. Direct sulphation of $CaCO_3$ to $CaSO_4$ showed to be an effective desulphurization process in the PFBC.

Further Zevenhoven *et al.*, (1998b), used a pressurized thermo gravimetric analyzer (P-TGA) to obtain a ranking of limestones and dolomites with known chemical composition and structural properties, by relating reactivity to the chemical and physical properties. The conclusion was that the sulphur capture properties of the different adsorbents were sensitive to the changing structural properties occurring during the desulphurization process. This is in agreement with the results obtained by Alvarez and Gonzalez, (1999) and Dam - Johansen and Ostergaard, (1991) who evaluated many other limestones and dolomites.

Wang *et al.*, (2002) used modified limestone to investigate the sulphation process. It was concluded that modified limestone is more effective compared to natural limestone. Cigdem *et al.*, (2001) used soda ash (Na_2CO_3) as the adsorbent agent for the SO_2 adsorption, a high conversion of Na_2CO_3 to Na_2SO_3 was observed compared to the conversion of Ca – based adsorbents.

Zhang *et al.*, (2003) used a drop tube furnace to study sulphur capture capacities on sulphur removal. A high sulphur removal capacity was reported, resulting from the calcium acetate used. The high specific surface area of the calcium acetate caused a delay in the sintering process that occurs at higher temperatures of sulphation.

Fuertes *et al.*, (1995), using two different reactors: a thermo gravimetric system and a shock micro reactor studied the sulphation of dolomite particles at high CO_2 partial pressures, different temperature and with different particle size. Two reaction

stages were observed with a rapid reaction rate observed at the beginning of the reaction, which slowed down as the reaction continued. They reported the presence of diffusional effects, which are dependant on the particle size.

2.4.1 Reaction rate models

The modelling of the overall reaction involving desuphurization has received extensive attention by many investigators in order to elucidate the many mechanisms involved.

Various models have been evaluated to describe the sulphation of limestone and dolomite. These include the random pore model (Bhatia and Perlmutter, 1980), the grain model (Hartman and Coughlin, 1976; Borgwardt *et al.*, 1987), partially sintered grain model (Linder and Simonsson, 1981), pore plugging model (Simons and Garman, 1986) and the grain-micrograin model (Dam - Johansen *et al.*, 1991). Many models are concerned with the gradual change of the physical structure as the product layer develops in the porous structure. A number of sulphur capture models, have been proposed by Lyngfelt and Leckner, (1999) based on similar basic assumptions. Publications describing the unreacted shrinking core (USC) model with modifications are numerous and some are discussed as follows

Alvarez and Gonzalez, (1999) using the USC model reported that the reaction kinetics is controlled by both chemical reaction and product layer diffusion. The activation energy of 87.2 kJ/mol was reported, and the effective diffusivity varied between 4×10^{-9} and 9×10^{-9} cm^2/s. A satisfactory result was obtained when the term expressing the product layer diffusion coefficient as a function of conversion was introduced.

Zevenhoven *et al.*, (1998a and 1998b) used the USC model and came to the conclusion that the conventional USC modelling does not allow for the explanation of the differences in the conversion of chemically similar but physically different limestone and dolomite. An alternative model termed unreacted shrinking core model with variable effective diffusivity (USC – VED) was developed, including the structural parameters of the adsorbent. The results showed that the variable

effective diffusivity leads directly to a conversion dependent on the Thiele modulus, with a shift with regard to the rate determining mechanism. The apparent activation energy for the chemical reaction was found to be 79.9 kJ/mol and the product layer diffusivity of the order of 10^{-10} (m^2/s).

Trikkel and Kuusik, (2003), applied the USC - VED model, and reaction rate constants of 2.6×10^{-3} to 6.8 m/s, product layer diffusion in the range of 3.26×10^{-10} to 8.3×10^{-9} m^2/s were reported. At atmospheric pressure the assumption was made that chemical kinetics initially controlled the rate followed by intra particle diffusion. However, at a high pressure chemical kinetics and diffusion control mechanisms occurred during the initial stages of the reaction.

2.5 Experimental equipment

The most used laboratory reactor for desulphurization studies is the TGA with fewer studies involving the drop tube furnace and laboratory scale fluidized beds (Table 2.4). Comparisons of the results obtained from different laboratory reactors were reported (Dam - Johansen and Ostergaard, 1991; Yrjas *et al.*, 1995) and it was deduced that results from a TGA are suitable for evaluating the performance of adsorbents with respect to chemical kinetics (intrinsic) and particle diffusion for FBC development. The main disadvantage of the TGA is that because of the low gas conversion per pass, it is not possible to assess the gas product composition accurately.

Table 2.4: Experimental conditions used by other investigators in laboratory studies on the adsorption of SO_2 with Ca-based adsorbents.

Investigator	Material	Particle Size(μ m)	SO_2 conc.(ppm)	Temperature (°C)	Pressure (bar)	Experimental Apparatus
Yrjas *et al.*, (1995)	Limestone, Dolomite	200 - 400	3000	850 - 950		P - TGA
Wang *et al.*, (2002)	Limestone, Na_2CO_3	31.4	3000	900		TGA
Garcia *et al.*, (2002)	$Ca(OH)_2$ derived CaO			300		TG-DTA
Zevenhoven *et al.*, (1998)	Limestone, Dolomite	250 - 300	3000	850 - 950	15	P - TGA
Alvarez & Gonzalez, (1999)	Limestone, Dolomite	100 -200, 500 - 595	5000	800 - 925	12 & 15	P - TGA
Iisa *et al.*, (1991)	Limestone					P - TGA
Chiung *et al.*, (2004)	$Ca(OH)_2$ /fly ash		1000	60	1	TGA
Mahesh *et al.*, (2004)	Limestone		3000	700	1	TGA
Trikkel & Kuusik, (2003)	Limestone	120 - 160	5000	850	1 & 15	TGA
Zhang *et al.*, (2003)	Limestone			1100 - 1400		Drop Tube Furnace

CHAPTER 3
MODELS EVALUATED

3.1 Introduction

This chapter gives the description and detailed derivation of the models used in this study. From the kinetic models reported in Section 2.4.1, the unreacted shrinking core model was selected to describe the experimental results. The kinetics of conversion is described both in terms of reaction kinetics and diffusion. Section 3.2 gives a description and the equations of the model.

3.2 Models evaluated

The basic particle model that is used in this study is the unreacted shrinking core (USC) model, which is extended to the unreacted shrinking core model with variable effective diffusivity (USC - VED). Both models are presented in sections 3.2.2 and 3.2.3, and are similar to the models presented by Zevenhoven *et al.,* (1998b).

3.2.2 Unreacted shrinking core model

3.2.2.1 Description

The USC model assumes that, each particle is considered to be spherical and that it maintains this form during reaction. There exist a sharp interface separating solid products and reactants in the particle. The reactive gas diffuses into the layer of products up to the interface and then reacts. During reaction, the interface moves towards the centre of the particle keeping its initial form. The porosity of the particle as well as the number of pores remains constant during reaction. The structural change of the particle due to chemical reaction results only in the expansion or shrinking of the particle. In the particle, gas diffuses in the radial direction.

3.2.2.2 Derivation of equations

The USC conversion - time model equations for the combination of reaction kinetics and intra - particle diffusion gives the following relation between time and overall conversion, involving surface reaction and diffusion through the product layer (combine rate controlling mechanisms)(Carberry, 1976).

$$t = \tau_R F_R(X) + \tau_D F_D(X) \tag{3.1}$$

With the functions $F_R(X)$ and $F_D(X)$ defined as:

$$F_R(X) = 1 - (1 - X)^{2/3} \tag{3.2}$$

$$F_D(X) = 3\left(\frac{Z - (1 + ZX - X)^{2/3}}{Z - 1} - (1 - X)^{2/3} \right) \tag{3.3}$$

In which Z is the ratio of molar volumes of product and reactant. If first order kinetics in SO_2 is assumed, τ_R and τ_D are given by:

$$\tau_D = \frac{R_{p_o}{}^2 \rho_{mol}}{6 D_{eff} c_g} \tag{3.4}$$

and:

$$\tau_R = \frac{R_{p_o} \rho_{mol}}{k_s c_g} \tag{3.5}$$

The USC - model described above is a useful tool in the description of gas - solid reactions, but is limited to processes where the ratio of reaction rate to diffusion rate does not change with conversion. This is, however, not the case in reactions where the internal structure changes, *e.g.* in the sulphation of CaO.

Therefore, Zevenhoven *et al.*, (1998b) and Zevenhoven *et al.*, (1996) refined the USC - model to the USC - VED model, which is presented in the next section. A similar approach of combining pore diffusion and solid - state (product) diffusion in a single diffusion coefficient, has also been used by Fernouli and Lynn, (1995), for the sulphation of limestone.

3.2.3 Unreacted shrinking core model with variable effective diffusivity

3.2.3.1 Description

The unreacted shrinking core model with variable effective diffusivity model (USC – VED model), implicitly accounts for changes in the internal structure of the adsorbent particles during conversion. These changes can cause the ratio of the reaction kinetics to diffusion rate, hence the Thiele modulus, to change with conversion. The most important derivations and equations are given in Section 3.2.3.2 and are based on the results published by Zevenhoven *et al.*, (1998b) for calcium carbonate sulphation.

3.2.3.2 Derivation of equations

The effective diffusivity (D_{eff}) accounts for all diffusion effects inside the particle. In the case of the sulphation of CaO, the two most important transport resistances are (i) diffusion in the pores and (ii) diffusion through the product layer (Zevenhoven *et al.*, (1998b). From a mechanistic view, these resistances can be modelled in series, which will result in the following equation.

$$\frac{V_p + V_{pl}}{D_{eff}} = \frac{V_{pl}}{D_{pl}} + \frac{V_p}{D_p} \qquad (3.6)$$

The volume fractions of the product layer (V_{pl}), pores (ε) and unreacted material (V_u) can be calculated with equations. 3.7 - 3.9 respectively:

$$V_{pl} = (1 - \varepsilon_o) XZ \qquad (3.7)$$

$$\varepsilon = \varepsilon_o - (1-\varepsilon_0)(Z-1)X \tag{3. 8}$$

$$V_u = (1-\varepsilon_0)(Z-1)X = 1 - V_p - V_{pl} \tag{3. 9}$$

The diffusion in the pores of the particle can be expressed in terms of the molecular diffusion coefficient (D_m) and the Knudsen diffusion coefficient (D_K) inside a porous structure with porosity (ε) and tortuosity (τ) according to:

$$\frac{1}{D_T} = \frac{1}{D_m} + \frac{1}{D_K} \tag{3.10}$$

where D_K is determined by (Do, 1998) :

$$D_K = \frac{2}{3}\bar{r}_p\sqrt{\frac{8RT}{\pi Mm}} \tag{3.11}$$

and D_m is calculated via the semi-empirical relation of Fuller *et al.*, (1966):

$$D_m = \frac{10^{-3}T^{1.75}\sqrt{Mm}}{P\left(V_A^{1/3} + V_B^{1/3}\right)^2} \tag{3.12}$$

The effective diffusion coefficient in the pores, in the absence of a product layer resistance, can be expressed as (Neomagus *et al.*, 2000)

$$D_{eff} = \frac{\varepsilon}{\tau}D_p \tag{3.13}$$

If a product layer is formed, the conversion dependant effective diffusion coefficient can be derived from equations. 3.6 to 3.13 as:

$$D_{eff}(X) = \frac{\varepsilon_o + (1-\varepsilon_o)X}{\frac{\tau}{D_T} + \frac{Z(1-\varepsilon_o)X}{D_{pl}}} = D_{eff,o}\frac{1+AX}{1+BX} \tag{3.14}$$

Where A and B are given by:

$$A = \frac{1-\varepsilon_o}{\varepsilon_o} \quad , \; B = \frac{(1-\varepsilon_o)ZD_p}{3D_{pl}} = \frac{AD_{eff,o}Z}{D_{pl}} \tag{3.15}$$

Since initially (at t = 0) no product layer has formed, $D_{eff,0}$ can be described as:

$$D_{eff,o} = \frac{\varepsilon_o}{\tau} D_p^0 \tag{3.16}$$

The USC - VED can now be described similar to Equation 3.1, and will be used in the analysis of the experimental results.

$$t = \tau_R F_R(X) + \tau_{D,o}\frac{1+BX}{1+AX}F_D(X) \tag{3.17}$$

In this equation, τ_R and B are the only unknown parameters and can be regressed using the experimental results. The regressed value of τ_R will give the reaction kinetic constant k_s, and B will result in a numerical value of the diffusion coefficient in the product layer, D_{pl}. From these values, the conversion dependent Thiele modulus $\phi(X)$ can now be calculated according to:

$$\phi(X)^2 = \frac{\tau_D(X)}{\tau_R} = \frac{R_{p_o}k_s}{6D_{eff}(X)} = \frac{R_{p_o}k_s}{6D_{eff,o}}\left(\frac{1+BX}{1+AX}\right) = \tau_{D,0}\left(\frac{1+BX}{1+AX}\right) \tag{3.18}$$

CHAPTER 4
EXPERIMENTAL

4.1 Introduction

A description of the experimental apparatus, experimental methods and materials used in this study are given in this chapter. Section 4.2 gives an outline of the experimental lay – out with a detail description in Section 4.2.1 of the high-pressure thermo gravimetric analyzer (HP-TGA) used. The materials used in this investigation are described in Section 4.3 with a brief description of the methods used to characterize the adsorbents provided in Section 4.3.1. Other materials such as gases are also described in Section 4.3.2 and experimental conditions and procedure are discussed in Section 4.4.

4.2 Experimental Apparatus

The experimental apparatus used for this study is a thermo gravimetric analyzer (TGA) to obtain the reactivity performance of different adsorbents. The experimental flow sheet consists of the following key components, furnace, gas supply, microbalance, data acquisition, pressure control and the TGA (Figure 4.1). The microbalance, which is mounted on top of the reactor provides the measurement of the mass change, which the sample in the TGA undergoes. A typical gas supply network is shown in Figure 4.1, which is used to supply reaction gases and to control the flow rates using very accurate mass flow controllers (Brooks type). The pressure in the TGA is accurately controlled with the necessary control valves and the experimental results are logged by means of an on - line computer system.

4.2.1 Description of TGA

The TGA used in this work is a Berggbau - Forshung GMBH, 1987 model supplied by Deutsche Montan Technology, DMT, Germany (Figure 4.1). The microbalance is housed in the reactor chamber and is protected from any corrosive reacting gases with an inert gas purge. The sample holder (basket) shown in

Figure 4.2, which is suspended from the microbalance with a stainless steel chain, has a cylindrical shape, with the samples packed evenly between an inner stem and an outer gauze. The basket is made of stainless steel and the sieve of platinum and is capable of being loaded with solid particles with a maximum diameter of 5mm and a total mass of 800 mg

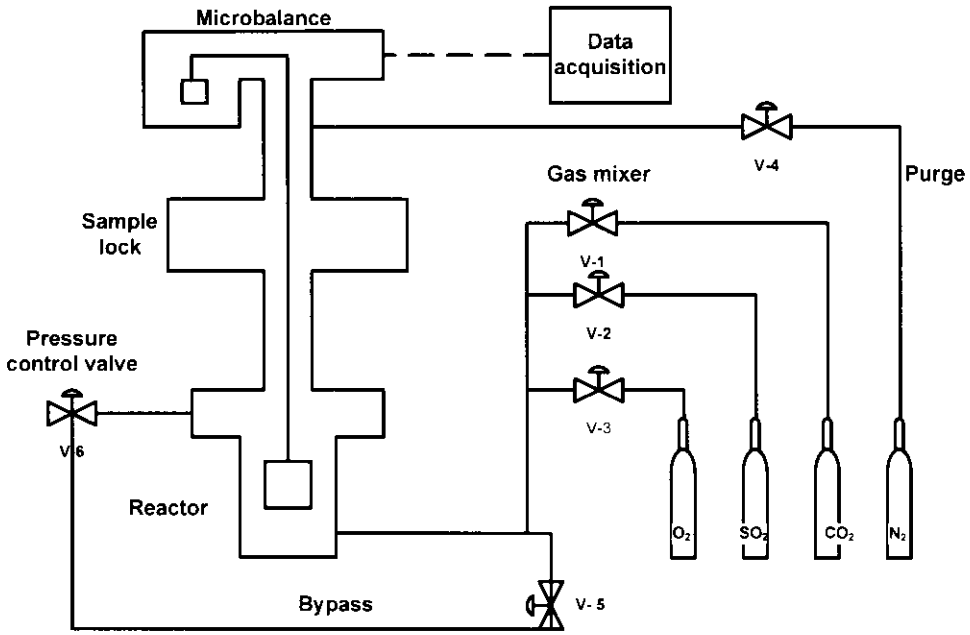

Figure 4.1: Schematic diagram for the experimental lay out.

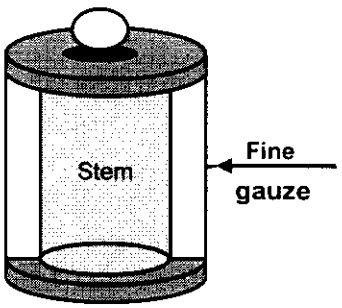

Figure 4.2: Sample holder.

The reactor pressure vessel is made of stainless steel and is designed to be operated at a maximum temperature of 1100^{O}C at a pressure of 100 bar. A thermocouple (J type) is placed a few millimetres beneath the sample holder to record the reaction temperature (with an accuracy of ± 2°C), which is controlled with a temperature controller. The temperature controller is capable of generating a linear heating rate of up to 100°C/min. A sample lock between the balance and reactor is provided, which is equipped with an electrical driven winch system allowing lowering and lifting of the sample basket. A photograph of the TGA is given by in Figure 4.3.

4.3 Materials

4.3.1 Adsorbents

The adsorbents (dolomite A and dolomite B) used in this study originated from a South African dolomite mine and were supplied by Eskom, which are also used by their research division concerning the development of FBC. These samples were screened to a particle size of 214 – 300 μm and were used for all characterization and reactivity measurements. Structural properties such as density, specific surface area, pore volume and images (meaningful) of the adsorbents were considered important properties for this study and were measured using the equipment and methods described as follows:

Chemical Composition:

The chemical (elemental) composition analysis of dolomite samples were carried out by Mintek (Johannesburg, South Africa) using inductive coupled plasma optic emission spectrometer (ICPOES).

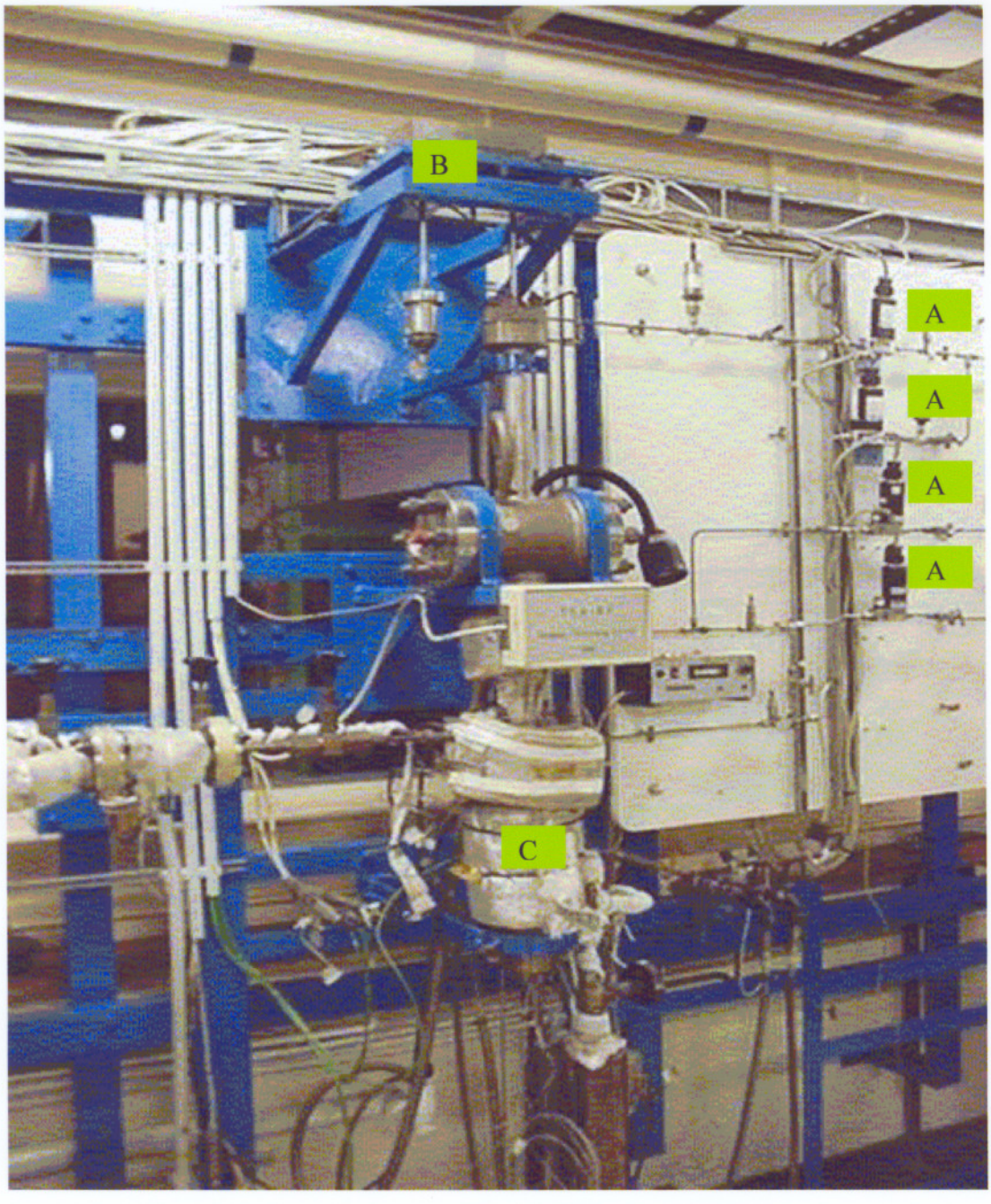

Figure 4.3: Thermo gravimetric Analyzer

A - mass flow controllers

B - mass balance

C - reactor

Structural Properties:

The following instruments available on campus were used:

(1) Micromeritis ASAP 2010 Analyzer

The specific surface area was measured using a Micromeritis ASAP 2010 Analyzer. With a BET adsorption technique, the pores were characterized by adsorbing nitrogen, at liquid nitrogen temperature (-196°C). The method is used for the determination of pore diameter range of 0.0004 – 0.5 μm (Stanely - Wood and Lines, 1992). With this method using nitrogen, it is possible to calculate the meso - pore size distribution (2 – 50 nm) and to determine the micro - pore volume (<2 nm) only. In the context of adsorption, it is useful to classify porous solids in terms of their pore widths with micro - porous solid with pores of widths <2 nm, meso - porous solid with pore widths in the range of 2 – 50 nm, and macro - porous with pores width >50 nm.

(2) Micromeritis AutoPore Analyzer III

The porosity was measured using a Micromeritis AutoPore Analyzer III. The mercury intrusion technique involves filling the pores with mercury under pressure. The pressure applied being a function of the pore entrance diameter and the volume of the mercury intruded being taken as representing the volume of the pore of that diameter. The method is suitable for materials with pores in the approximate diameter range of 0.003 – 400 μm (Stanely - Wood and Lines, 1992).

(3) Helium Pycnometer

The density of the particles was measured using a helium pycnometer (quantachrome). The sample was placed in the sample chamber of a helium pycnometer, and the particle bulk density was determined from the volume of voids within the particles

(4) Scanning Electron Microscope (SEM).

The scanning electron microscopy (FEI quanta 200) was used to obtain images of the morphology of the dolomite surfaces (Allen, 1990). In SEM a fine beam of electrons of medium energy (5 – 50kV) is caused to scan across the sample in a series of parallel tracks. These electrons interact with the sample producing secondary electron emission (SEE), back - scattered electrons (BSE), light or cathodoluminescence and X – rays. Each of these signals can be detected and displayed on the screen of a cathode ray tube like a television picture Final results are generally presented in photographic form.

4.3.2 Gases

The gases used in this study are pure nitrogen and carbon dioxide and two different sulphur dioxide mixtures. Nitrogen was used as the inert gas.

The specifications of different gases used are as follows:

Nitrogen	High purity > (99.99%)
Carbon dioxide	High purity > (99.99%)
Sulphur dioxide mixtures	(i) 3000 ppm SO_2, 20% CO_2, 4% O_2, balance N_2
	(ii) 3000 ppm SO_2, 8% CO_2, 8%O_2, balance N_2.

All these gases, were supplied by Afrox (Johannesburg)

4.4 Experimental Procedure

All experiments were carried out at atmospheric pressure (0.875 bar) following calcination with pure nitrogen with gas mixtures that were prepared on - line from different calibrated mixtures contained in bottles linked to the a manifold system. The mass of sample in the sample basket was ± 500 mg and the total gas flow rate through the dolomite samples was 1000 ml/min sufficient to ensure the absence of mass transfer resistance to the particle surface (film diffusion). The operation of the TGA is considered to be equivalent to a differential reactor. Each experiment consisted of (1) an initial heating period with flowing nitrogen with the basket suspended above the furnace (cold) (2) calcination following lowering of sample

basket into the hot furnace with flowing nitrogen, and (3) reaction following switch over from nitrogen to the desired gas mixture. The mass of the sample was recorded continuously during all the stages. A list of the experiments performed is given in Chapter 5 (Table 5.3), which were carried out under conditions very similar to FBC conditions. Many experiments were repeated to confirm reproducibility and it was found that the error associated with the final results (mass) were within 5%.
Results consisting of fractional mass increase and percentage conversion of CaO to $CaSO_4$ are presented with the latter calculated according to equation 4.1 (Irfan and Balci, 2002)

$$X = \frac{(M_t - M_0)/Mm_{SO_3}}{(x_{CaO} M_0)/Mm_{CaO}} \qquad (4.1)$$

M_0 is the mass of sample after calcination, M_t is the mass of sample at any time , x_{CaO} is the mass fraction of CaO in the sample after calcination , Mm_{SO_3} and Mm_{CaO} are molecular mass of SO_3 and CaO respectively.

CHAPTER 5
RESULTS AND DISCUSSION

5.1 Introduction

This chapter presents the results obtained in this study consisting of characterization, reactivity measurements and modelling (Everson *et al.*, 2005). Section 5.2 gives the results of the characterization of adsorbents used, which are referred to as dolomite A and dolomite B. Sulphation and recarbonation results with CaO are discussed in Section 5.3. Section 5.4 gives modelling results using unreacted shrinking core model with and without a variable effective diffusion coefficient, as a result of molar density changes, to describe the reaction kinetics of SO_2 reaction with CaO.

5.2 Characterization

Chemical and physical properties of dolomite A and dolomite B were characterized to get a better understanding regarding of especially structural effects which have an effect on the reaction characteristics and on the mechanisms describing the model. The characterization and experimental procedures are discussed in Chapter 4 and details of the modelling in Chapter 3.

5.2.1 Elemental analysis of original adsorbents

The elemental analysis results of dolomite A and dolomite B tested are shown in Table 5.1. With regard to the calcium and magnesium oxide (equivalent) it can be seen that there is a significant difference, with dolomite A having a CaO/MgO ratio of 4.05 and dolomite B having an equivalent ratio of 1.47. The presence of magnesium oxide can only have a structural effect since it does not react with SO_2 at FBC conditions (Zevenhoven *et al.*, 1998(b), Alvarez and Gonzalez, 1999). Both dolomite A and B were found to have a higher concentrations of manganese, iron and silicon (however small) when compared with most limestones and dolomites used by Yrjas *et al.*, (1995).

Table 5.1: Elemental analysis of dolomite A and dolomite B (wt.%)

Adsorbets	C	Si	Al	Fe	Mn	Ti	Mg	Ca	[a]CaO	[a]MgO	[a]$CaCO_3$	[a]$MgCO_3$
Sample A	11.2	2.84	0.32	1.56	0.3	<0.05	5.58	26.9	37.7	9.3	67.3	19.5
Sample B	12.8	1.43	<0.05	0.59	0.5	0.05	11.5	20.2	28.3	19.2	50.5	40.3

a - calculated from elemental analysis

5.2.2 Structural analysis

Adsorption isotherms obtained from BET measurements using nitrogen are shown for both dolomites in Figure 5.1. These results are characteristic of adsorption isotherms Class I and Class IV according to the classification given by Gregg and Sing, (1982) which indicate that both dolomites consists of micro - and meso – pores. The porosities reported include the meso - and macro pores only as determined by mercury intrusion.

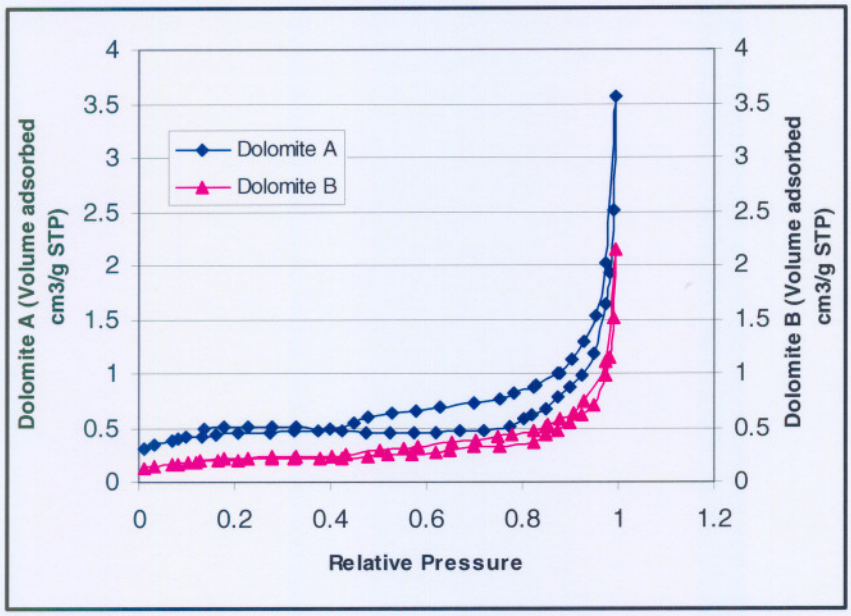

Figure 5.1: BET – isotherms

The most important structural parameters from the BET analysis, the mercury prorosimetry, and the helium pycnometer are given in Table 5.2. The BET surface area and pore volume of dolomite A are higher compared to dolomite B and the BET surface areas of both samples are slightly lower than that reported for many limestones and dolomites examined in the literature while the pore diameters are larger (Zevenhoven *et al.*, 1998b).

Table 5.2: Structural properties of dolomite A and dolomite B

Adsorbents	[a]Particle Density (kg/m^3)	[b]BET surface area (m^2/g)	[b]Pore volume (cm^3/g)	[c]Average Pore diameter (μm)	[c]Porosity (-)
Dolomite A	2981	1.5	0.0025	1.496	0.227
Dolomite B	3037	0.7	0.0015	1.416	0.282

a – obtained from helium pycnometer (bulk density)

b – obtained from BET

c – obtained from mercury intrusion

5.2.3 SEM micrographs

Scanning electron microscope micrographs were determined to investigate any surface structural changes of the adsorbents as a result of calcination and reaction and results are shown in Figure 5.2. Results of the original adsorbents and the corresponding adsorbents after sulphation (and recarbonation) reactions at 750°C and 950°C with 25% CO_2 are shown. These SEM micrographs show that surface thermal cracks developed as a result of the thermal treatment (thermal shock) have increased with temperature and they only appear on the surface (limitations of measurements). This behaviour is difficult to model and was not attempted in this investigation. The results presented also include the effects of phase changes ($CaCO_3$, CaO and $CaSO_4$) resulting in narrowing of pores, which is not visible with the magnification used.

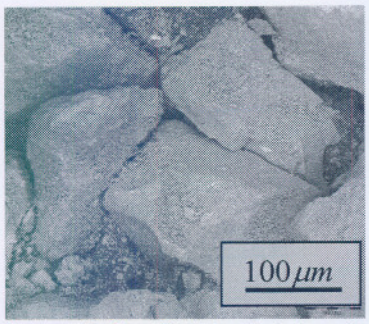

Figure 5.2a: Original dolomite A

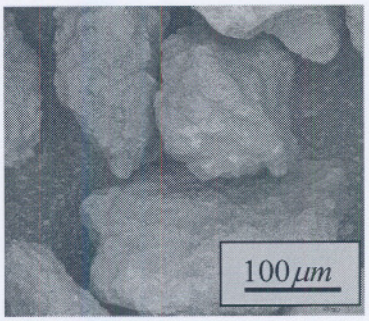

Figure 5.2b: Original dolomite B

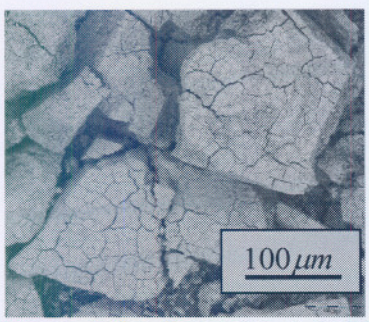

Figure 5.2c: Dolomite A at 750°C

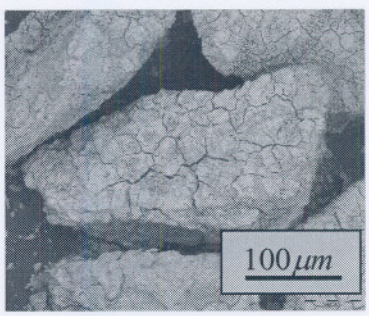

Figure 5.2d: Dolomite B at 750°C

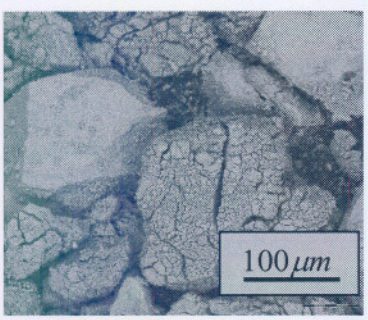

Figure 5.2e: Dolomite A at 950°C

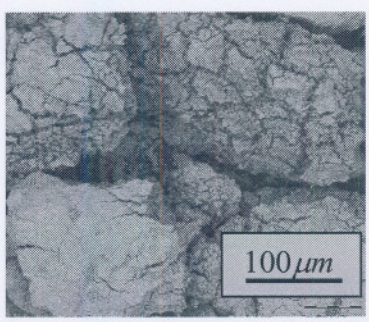

Figure 5.2f: Dolomite B at 950°C

Figure 5.2: SEM micrographs of dolomites A and B before and after reaction at 750°C and 950°C.

5.3 Experimental reactivity results

5.3.1 Introduction

SO_2 capture with CaO under atmospheric pressure was the main objective of this study and for this purpose experimental conditions were initially determined to ensure that no recarbonation of CaO to $CaCO_3$ occurred. This result was also compared with theoretical results for pure calcium compounds in order to demonstrate the effect of the mineral form of the reactive calcium carbonate/oxide. Experimental evaluation of the different dolomites, were then performed at conditions favouring the presence of CaO only. All experiments involved an initial calcination period and typical thermo gravimetric results showing calcination and sulphation and/of recarbonation are shown in Section 5.3.2. Recarbonation (absence of sulphation) results are given in Section 5.3.3, simultaneous recarbonation and sulphation in Section 5.3.4 and finally sulphation results in Section 5.3.5.

A list of the successful experiments conducted from which results were derived and reported in this dissertation are shown in Table 5.3 which can be summarized as follows:

(1) All sulphation/recarbonation experiments were done at atmospheric pressure (0.875 bar) with 2500 ppm SO_2 in CO_2, O_2 and N_2 mixtures at temperatures between 750°C and 950°C.

(2) Recarbonation experiments were done with CO_2/N_2 mixtures at temperatures between 750°C and 950°C also at atmospheric pressure (0.875 bar).

Table 5.3: Experiments conducted

Experiment Number	Adsorbent	Temp. (°C)	CO_2 (%)	CO_2 partial pressure (bar)	SO_2 (ppm)
OA1	Dolomite A	750	14	0.12	2500
OA2	Dolomite A	750	25	0.22	2500
OA3	Dolomite A	850	8	0.07	2500
OA4	Dolomite A	900	8	0.07	2500
OA5	Dolomite A	950	8	0.07	2500
OA6	Dolomite A	950	14	0.12	2500
OA7	Dolomite A	950	25	0.22	2500
OA8	Dolomite A	750	8	0.07	0.0
OA9	Dolomite A	950	25	0.22	0.0
OA10	Dolomite A	750	8	0.07	0.0
OA11	Dolomite A	800	8	0.07	0.0
OA12	Dolomite A	850	8	0.07	0.0
OA13	Dolomite A	900	8	0.07	0.0
OA14	Dolomite A	950	8	0.07	0.0
OB1	Dolomite B	750	14	0.12	2500
OB2	Dolomite B	750	25	0.22	2500
OB3	Dolomite B	850	8	0.07	2500
OB4	Dolomite B	900	8	0.07	2500
OB5	Dolomite B	950	8	0.07	2500
OB6	Dolomite B	950	14	0.12	2500
OB7	Dolomite B	950	25	0.22	2500
OB8	Dolomite B	750	8	0.07	0.0
OB9	Dolomite B	950	25	0.22	0.0
OB10	Dolomite B	750	8	0.07	0.0
OB11	Dolomite B	800	8	0.07	0.0
OB12	Dolomite B	850	8	0.07	0.0
OB13	Dolomite B	900	8	0.07	0.0
OB14	Dolomite B	950	8	0.07	0.0

5.3.2 TGA results

Typical thermo gravimetric results are shown in Figures 5.3 and 5.4 for dolomite A at 750°C with a mixture consisting of 2500 ppm SO_2, 25 % CO_2, 6.8 % O_2, and balance N_2 and at 950°C with a mixture consisting of 2500 ppm SO_2, 8 % CO_2, 6.8 % O_2, and balance N_2 respectively. The procedure consisted of calcination with pure nitrogen at the chosen temperature and the introduction of the reaction mixture after a constant mass was obtained during the calcination. The initial calcination period is characterized by a decreasing mass to a constant value and then followed by an increase in mass resulting from reaction involving recarbonation and sulphation (Figure 5.3) or sulphation only (Figure 5.4).

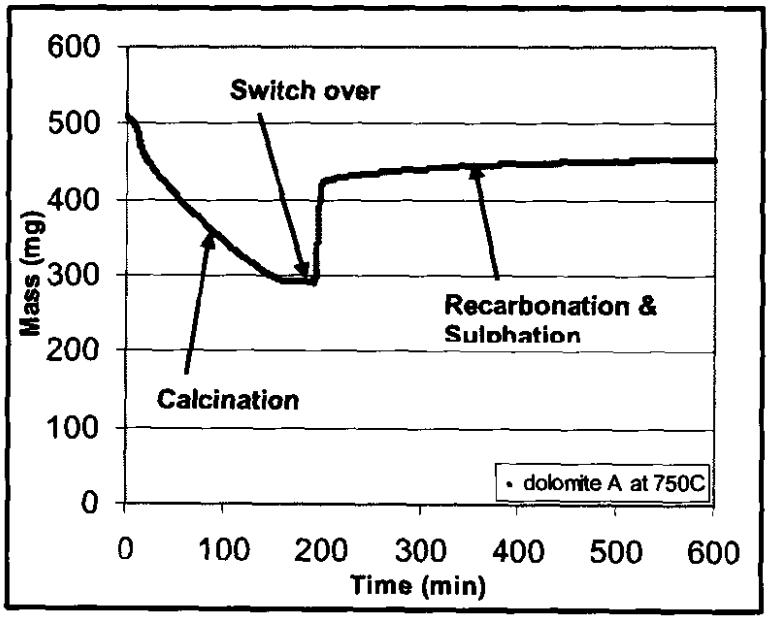

Figure 5.3: Calcination, recarbonation and sulphation at 750°C with 25 % CO_2.

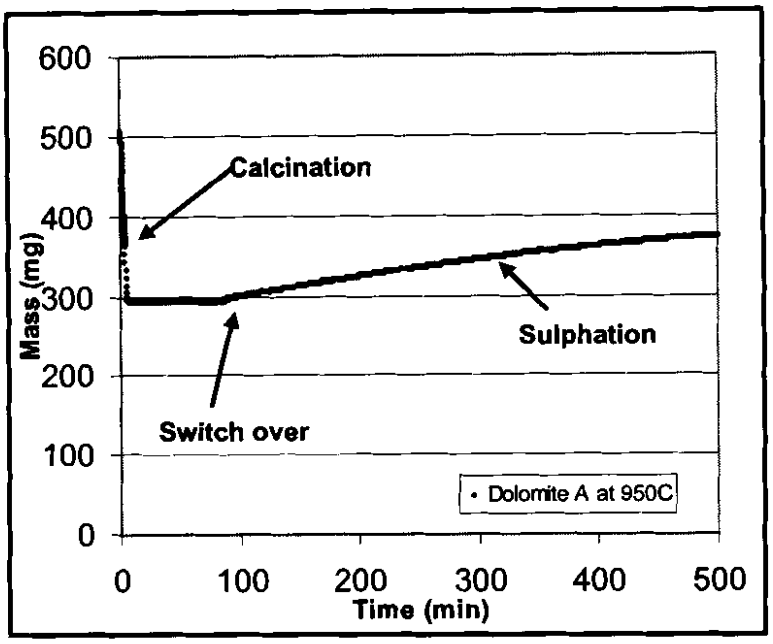

Figure 5.4: Calcination and sulphation at 950°C with 8 % CO_2.

5.3.3 Transition of CaO to $CaCO_3$

The determination of the region (temperature and CO_2 concentrations) for the preservation of the CaO phase (after calcination) during sulphation in the presence of CO_2 can be ascertained from a phase equilibrium diagram. However these results are for pure calcium compounds and needs to be checked for naturally occurring dolomites containing calcium in different mineralogical forms. Consequently, experiments with CO_2/N_2 mixtures only were carried out to determine conditions such that sulphation experiments with CaO occurred only, that is without recarbonation of the CaO. It should however be noted that $CaCO_3$ is also a good adsorbent for desulphurization.

Two sets of experiments with mixtures of 25% and 8% CO_2 with nitrogen are reported over a range of temperatures from 750°C to 950°C, which correspond to FBC conditions. These results were obtained following an initial calcination period with pure nitrogen at the reaction temperature. The results at the high concentration of CO_2 (25%) are shown in Figures 5.5 and 5.6 and for the lower concentration (8%) in Figures 5.7 and 5.8 for the two dolomites samples respectively.

The figures consist of plots of the fraction $\Delta M/M_O$ versus time with ΔM the increase in mass and M_O the mass after calcination. The conditions examined are also shown on the equilibrium diagram in Figure 5.9, which was calculated according to the procedure given in Appendix A. For the experiments with the 25% CO_2 mixture there was a large increase in mass at the lowest temperature of 750°C due to recarbonation to $CaCO_3$ and which is in agreement with the phase equilibrium calculation. At 950°C (far from the transition point) a very small increase in mass was observed (< 3%) which could be due to physical adsorption of CO_2 (high concentration) on the dolomite surface or some other unknown reactions occurring, but confirmation would require a more detailed study which was beyond the scope of this study (Yong and Rodrigues, 2002). The fractional mass change of the dolomites at 950°C is slightly larger for dolomite A when compare with dolomite B. This effect is also within the experimental error of the measurements.

For experiments with the 8% CO_2 mixture negligible mass increases were observed, that is no recarbonation, for experiments carried at 850°C, 900°C and 950°C which is in accordance with theory, whereas at 750°C and 800°C (close to transition point) significant recarbonation was observed (see Figure 5.9). The latter result (800°C) is a significant deviation from the theoretical result, which can be attributed to a mineral matrix effect. Deviations of this nature, have also been reported by other investigators (Tullin and Ljungstrom, 1989; Fuertes, *et al.*, 1995; Borgwardt, 1970).

From this study it is clear that sulphation of CaO in the dolomites examined occurs at conditions above the equilibrium transition temperature and below the equilibrium transition partial pressure and that for mixtures with low concentrations of CO_2, less than 8%, operating temperatures above 850°C will ensure the absence of recarbonation during the sulphation of CaO. This latter region was used to determine a reaction rate model for sulphation of CaO.

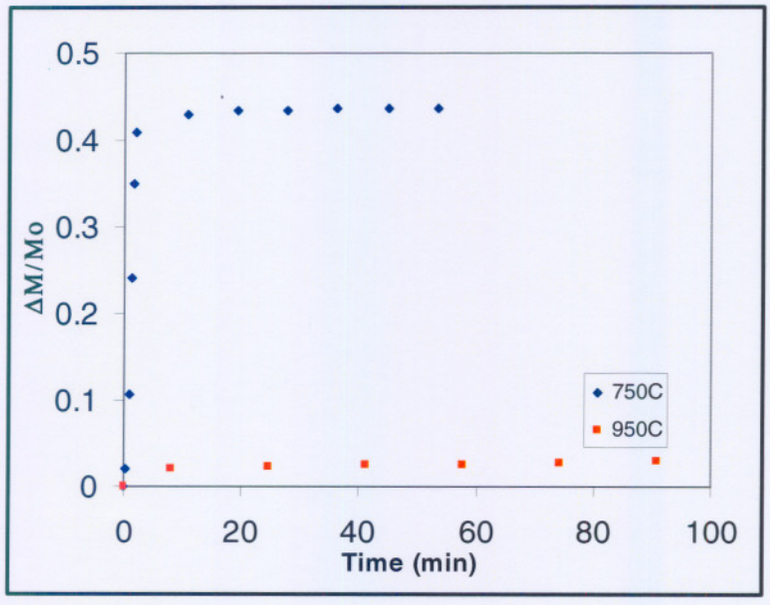

Figure 5.5: Recarbonation of dolomite A at 750°C and 950°C with 25 % CO_2

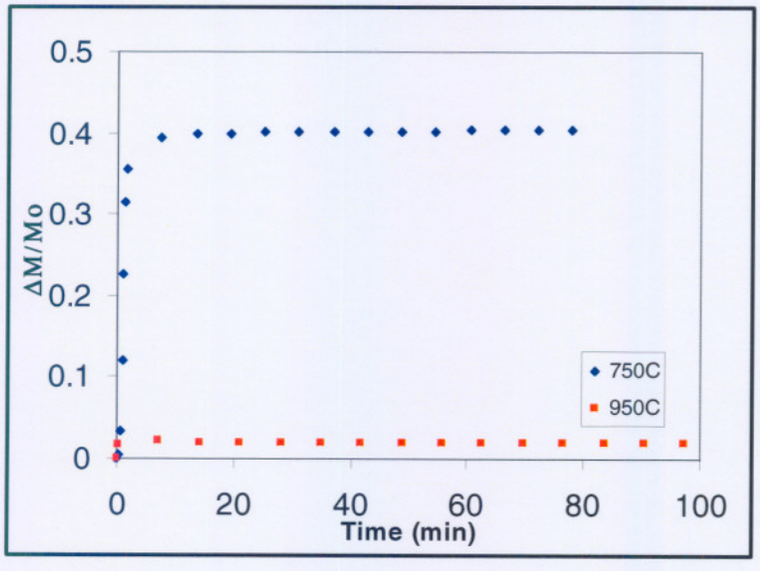

Figure 5.6: Recarbonation of dolomite B at 750°C and 950°C with 25 % CO_2

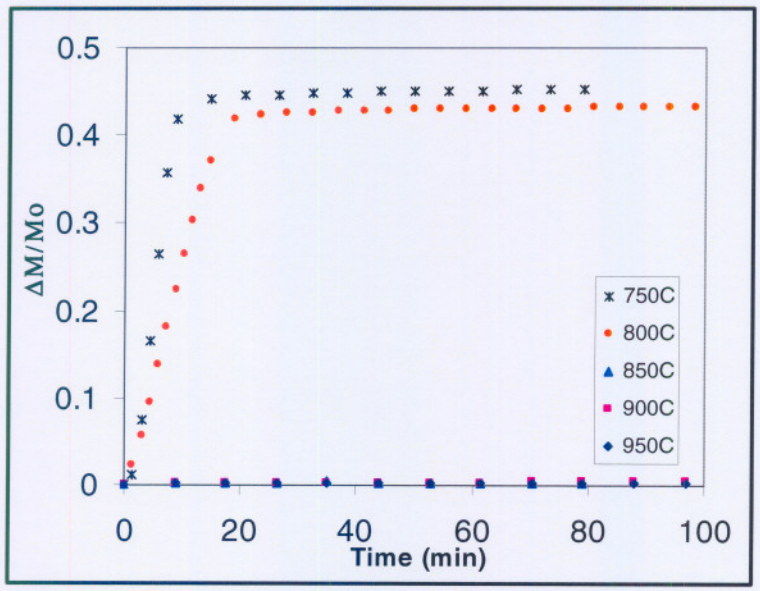

Figure 5.7: Recarbonation of dolomite A at different temperatures, with 8 % CO_2

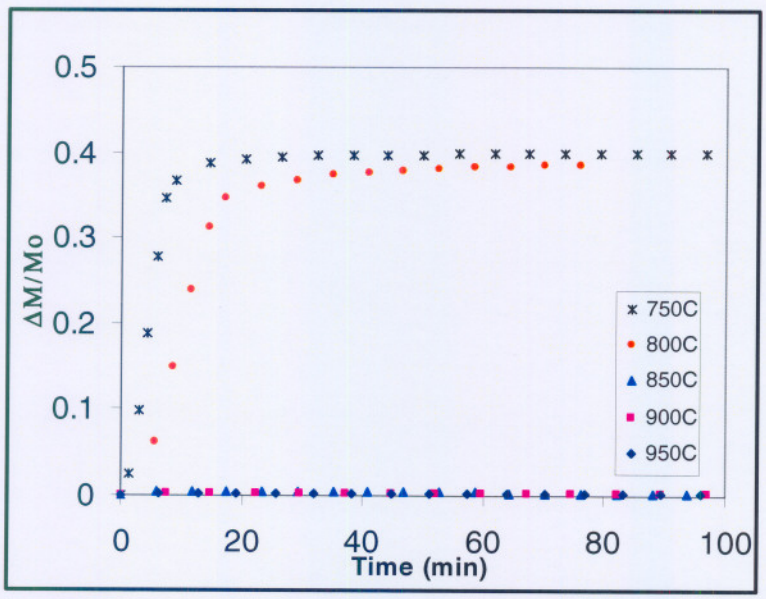

Figure 5.8: Recarbonation of dolomite B at different temperatures, with 8 % CO_2

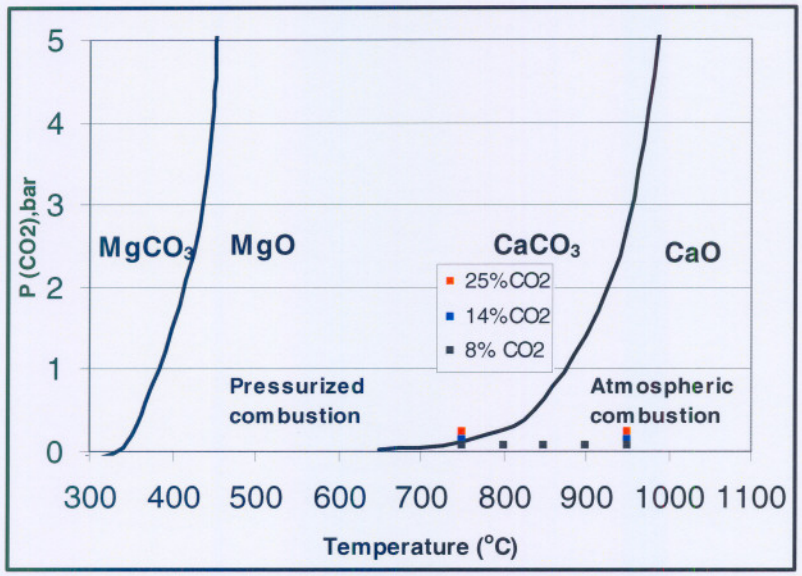

Figure 5.9: Thermodynamic equilibrium diagram .

5.3.4 Simultaneous sulphation and recarbonation

A comparison of recarbonation results as performed in the previous section with results involving both recarbonation and sulphation following calcination with nitrogen only, are shown in order to illustrate the effect of simultaneous formation of $CaCO_3$ under conditions favouring transformation of CaO. For the recarbonation experiment, a gas mixture of 25% CO_2 in nitrogen is used and for the recarbonation with sulphation experiments a gas mixture consisting of 2500 ppm SO_2, 25 % CO_2, 6.8 % O_2, and balance N_2 was used. Results from experiments that were carried out at 750°C following calcination with nitrogen at the same temperature are shown in Figure 5.10. It can be noticed that the reaction rates are initially very fast and similar, and are followed by a period with different reaction rates showing the effect of the presence of SO_2.

The chemical reactions occurring during the recarbonation and sulphation experiments are the following (Iisa, 1992).

1. Recarbonation of CaO

$$CaO + CO_2 = CaCO_3 \qquad \text{Reaction (1)}$$

2. Sulphation of $CaCO_3$

$$CaCO_3 + 0.5O_2 + SO_2 = CaSO_4 + CO_2 \qquad \text{Reaction (2)}$$

3. Sulphation of CaO

$$CaO + 0.5O_2 + SO_2 = CaSO_4 \qquad \text{Reaction (3)}$$

From the results obtained it is clear that reaction (1) is very fast and that it is possible that the contribution of reaction (3) to the overall sulphation is very small (Iisa, 1992). Since the relative amounts of different solid phases were not measured and because of many reactions participating, calculation of the sulphation reaction rate over CaO (alone) or $CaCO_3$ would be complex and not necessary since simpler methods are available. The capture of SO_2 with $CaCO_3$ (reaction (2)) in FBC (at high pressures) would not involve an initial calcination (starting with uncalcined dolomite) and thus no recarbonation, which is a much simpler process and has been investigated extensively by many researchers (Iisa, 1992; Zevenhoven *et al.*, 1998b; Tullin and Ljungstrom, 1989; Iisa and Hupa, 1990), while the capture with CaO could be carried out at higher temperatures at atmospheric pressures with no recarbonation (Ghardashkhani and Cooper, 1990; O'Neill *et al.*, 1976; Borgwardt, 1970). Research concerning the simultaneous occurrence of recarbonation and sulphation was undertaken by Tullin and Ljungstrom, (1989) and Iisa *et al.*, (1991)) who reported results involving measurement of the solid phases during the duration of the reaction. The results obtained from this study are in accordance with the results reported by these investigators.

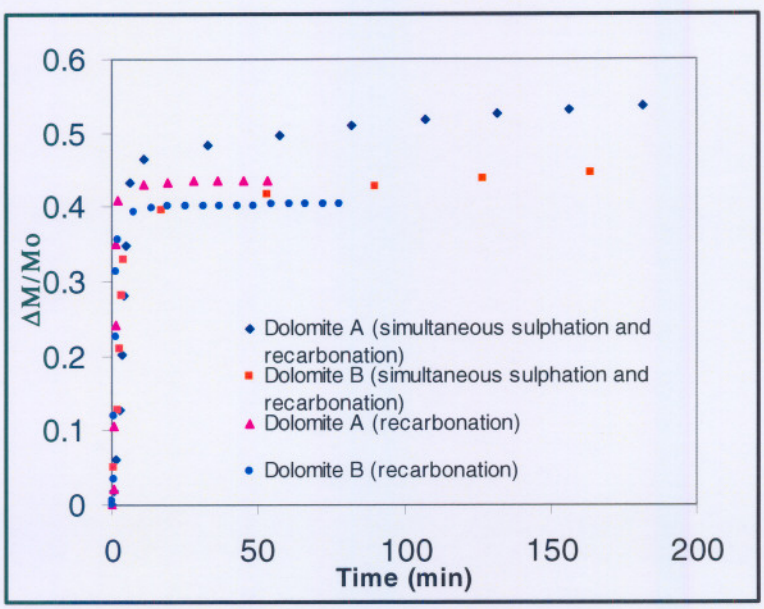

Figure: 5.10: Sulphation and recarbonation of dolomites A and B at 750°C

5.3.5 Sulphation

The objective of this section is to present sulphation reaction results involving CaO with a mixture consisting of 2500 ppm SO_2, 8 % CO_2, 6.8 % O_2, and balance N_2 at 850°C, 900°C and 950°C, which are similar to atmospheric pressure FBC conditions. The results are shown in Figures 5.11 and 5.12 for the two dolomites respectively. Experiments were conducted over much longer periods of time (500 minutes) than most results reported in the literature (<120 minutes) in order to establish whether any blocking (plugging) of pores occurred as a result of the molar volume increase resulting from the conversion of CaO to $CaSO_4$. All the results for dolomite A show a steady smooth increase over this period while the results for dolomite B at 850°C and 900°C have a slight break indicating some unusual change in the structure at nearly the same conversion (±18%). There appears to be no evidence of any extensive plugging during the reaction periods used for the two dolomites. Many results reported in the literature appear to reach a plateau after about 10 minutes and longer indicating a distinct closure of pores (Iisa and Hupa, 1990;Yrjas *et al.*, 1995; O'Neill *et al.*, 1976).

The initial reaction rates and conversions for the dolomites are very similar (< 20 minutes) with a difference evident at higher conversions as a result of essentially different structures developing, dependant on the composition and initial structural properties of the dolomites (Figure 5.13). Dolomite B (with a higher proportion of magnesium oxide) is slightly more active at corresponding temperatures for times less than ±300 minutes. The effect of magnesium oxide and impurities such as the iron oxides requires a more detailed study (with more samples) before any meaningful conclusions can be made. It was also found that the rate of sulphation was much slower than for recarbonation as reported above (Tullin and Ljungstrom, 1989).

The conversion levels attained after 120 minutes vary between 10% and 15% for the dolomites examined and are similar, except for the absence of a plateau, to results reported by Yrjas *et al.*, (1995) and Iisa and Hupa (1990). These researchers reported results for many limestones and dolomites at 1 bar pressure using a similar gas composition and some results at a temperature of 850°C showed a conversion

of just over 10%. There are however many limestones and dolomites reported in the literature that perform much better at atmospheric pressure, but insufficient characterization results are available in order to draw meaningful conclusions (Borgwardt, 1970; Ghardashkhani and Cooper, 1990; Iisa and Hupa, 1990; Yrjas *et al.* 1995; O'Neill *et al.* 1976). The conversion levels obtained with CaO are generally lower than for $CaCO_3$ with the latter occurring at higher pressures (Zevenhoven *et al.*,1998b). The results obtained in this study show that the reactivity characteristics of the dolomites are such that even after a long period of time (500 minutes) the sulphation rates are still significant which is indicative of the existence of open pores and that CaO conversions of 23% to nearly 40% (Figure 5.13) are obtained after 500 minutes of exposure.

It is clear from this study and from results in the literature that many variables affect the overall capture properties of the dolomites which include (1) structural properties such as particle size, porosity and pore structure dependant on dolomite mineral composition and the calcination conditions (Dam Johansen 1991, Yrjas *et al.*, 1995 and Irfan and Balci, 2002), (2) reaction kinetics dependant on pressure, temperature and SO_2 concentration (and solid phase present), (3) pore diffusion and diffusion through product layer, also dependant on the pressure, temperature, and relative molar densities of adsorbent and product, and (4) sintering at high temperatures of especially calcium oxide (Iisa and Hupa, 1990). Some of these variables such as the structural properties, consisting of particle size, porosity, relative molar densities and pore sizes (average), can be incorporated in a quantitative manner in a mathematical model to get a better understanding of the mechanisms involved. A mathematical model for the sulphation based on some characterization (determined and inferred) together with the experimental sulphation results is presented in the next section.

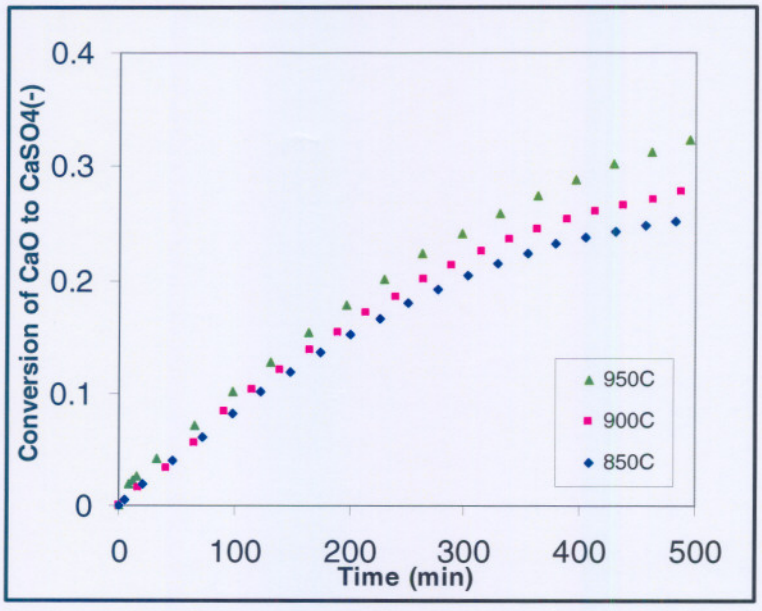

Figure. 5.11: Dolomite A: Sulphation at 850 to 950°C

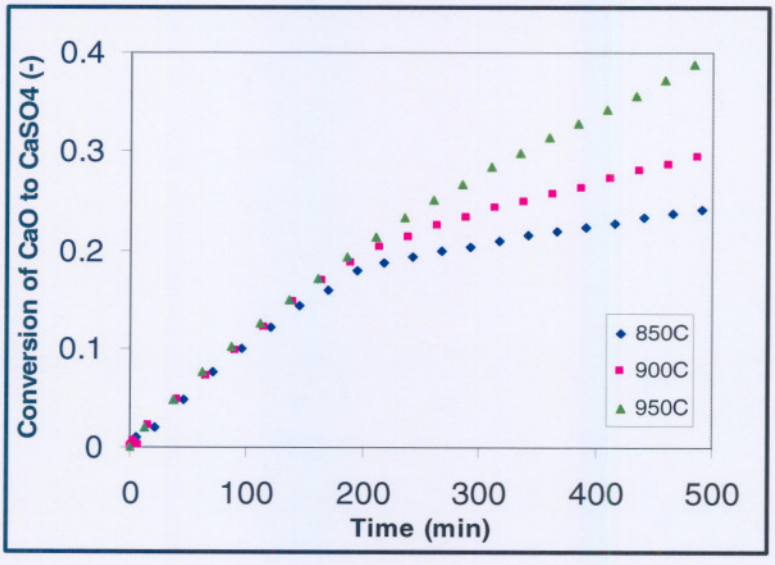

Figure 5.12: Dolomite B: Sulphation at 850 to 950°C

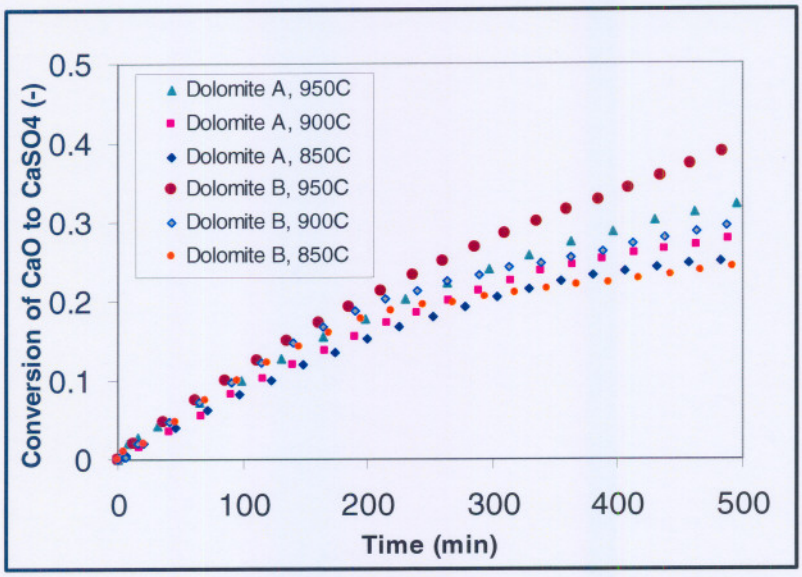

Figure 5.13: Comparison of sulphation performances of dolomites with 8% CO_2.

5.4 Modeling

5.4.1 Introduction

The unreacted shrinking core model with variable effective diffusivity, as described in Chapter 3, was used to model the experimental results. The experiments conducted under the gas atmosphere of 2500 ppm SO_2, 8 % CO_2, 6.8 % O_2 and balance N_2 at 850, 900 and 950°C were selected for modelling, since at these low partial pressures of CO_2 and high temperatures, the carbonation reaction is absent.

5.4.2 Input parameters of the model

The USC - VED model requires certain input parameters, which are described in this section. The molar volume ratio (Z) used was obtained according to equation 3.4 and is 2.73 for the conversion of CaO to $CaSO_4$, with the molar volumes of CaO and $CaSO_4$ being 16.9 cm^3/mol and 46 cm^3/mol respectively. The average particle radius $(R_{pa})$was taken as 140 μm, which is the average of the mesh size (214 - 350 μm) of the sieve used for screening. The tortuosity of the particle (τ) was taken as 3, which is a value typical for CaO (Zevenhoven *et al.*, 1998b). The porosity (ε) and average pore radius $(\overline{r_p})$ were determined from mercury intrusion as given in Table 5.2 and were assumed to remain constant during reaction. The SO_2 gas concentration (C_{SO_2}) was calculated with the ideal gas law at an atmospheric pressure of 0.875 bar. The numerical values for the molecular and Knudsen diffusivity were calculated from equation 3.11 and 3.12.

5.4.3 Numerical procedure

The rate parameters were determined according to the numerical procedure as described by Zevenhoven *et al.*, (1998b). τ_D and $D_{eff,o}$ were calculated according to equation 3.5 and 3.16 respectively. A was calculated from the initial porosity (ε_o), and the values of B and τ_R were fitted from the experimental results using

equation 3.17. From these fitted values, k_s and D_{pl} could be calculated from B and τ_R with equation 3.5 and 3.15 respectively.

5.4.4 Results

5.4.4.1 Comparison with the unreacted shrinking core model with variable effective diffusivity

A comparison of the experimental results and the USC – VED model is presented in Figure 5.14 for dolomite A. From this figure, it can be seen that the USC - VED model gives an accurate description of the experimental results. This result has not been previously published for calcium oxide sulphation.

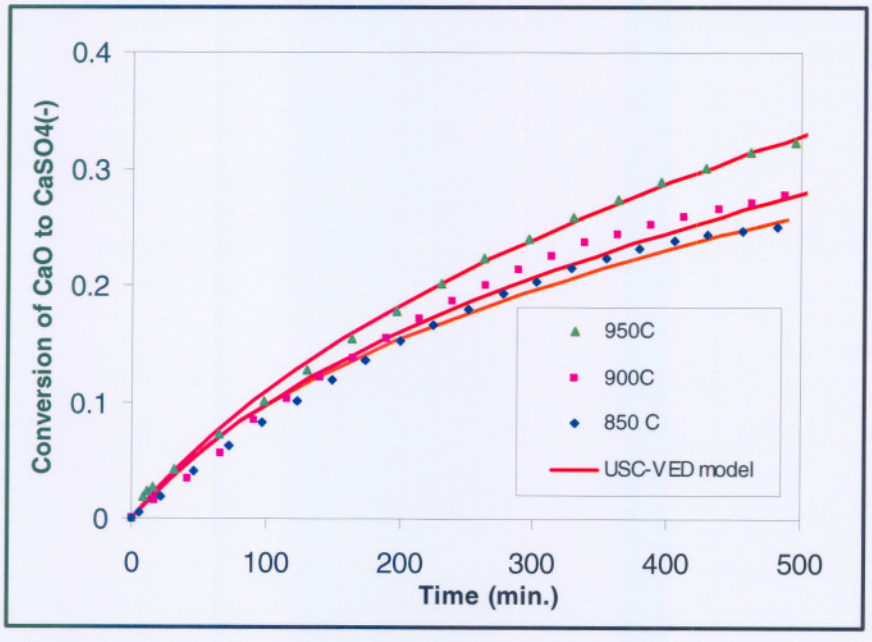

Figure 5.14: Dolomite A: Comparison of experimental data with calculated data (USC – VED) model

From the USC - VED model, the fitted parameters τ_R and B and the calculated values of k_s and D_{pl} are given in Table 5.4.

Table 5.4: Fitted and calculated values derived from the USC - VED model for dolomite A.

	850 °C	900 °C	950 °C
τ_R (min)	2397	2585	2310
B (-)	411	290	140
k_s (10^{-2} m/min)	4,86	4,91	5,50
D_{pl} (10^{-7} m^2/min)	7,70	10,70	19,10

It can be seen, from this table, that the kinetic constant (k_s) is only a slight function of temperature. Zevenhoven *et al.*, 1998(b) also reported a small temperature dependency of the kinetic constant. On the other hand, the diffusivity in the product layer (D_{pl})) strongly increased with temperature. This is also illustrated by the Thiele modulus as a function of conversion, which is given in Figure 5.15. The Thiele modulus increases with conversion, hence the reaction to diffusion rate increases, mainly due to the formation of the product layer, which forms an additional resistance to mass transfer. From Figure 5.15 it can also be derived that the Thiele modulus varies from about 0 to more than 2 (in the case of 850°C), which indicates a change from reaction controlled to a combination of reaction and diffusion controlled, a phenomenon that cannot be account for in the traditional USC - model.

The comparison of USC – VED results for dolomite A and results obtained by Zevenhoven *et al.*, 1998b are given in Table 5.5. From the different adsorbents used by Zevenhoven *et al.*, 1998b, dolomite sibbo was selected for comparison due to its similarity in chemical composition. The results in Table 5.5 confirm that the rate constant is independent of temperature, which was also reported by Amand *et al.*, (1986). The strong influence of temperature on the product layer diffusion coefficient, is also found by Zevenhoven *et al.*, (1998b).

Table 5.5: Comparison of USC – VED results for dolomite A and results obtained by Zevenhoven *et al.*, 1998b.

	850°C		950°C	
	Dolomite Sibbo	Dolomite A	Dolomite Sibbo	Dolomite A
$k_s\left(10^{-2} m/\min\right)$	8.40	4.86	9.24	5.50
$D_{pl}\left(10^{-7} m^2/\min\right)$	0.11	7.70	2.03	19.10

From the values of the diffusivity in the product layer, as given in Table 5.4 an Arrhenius graph can be obtained as given in Figure 5.16. From this figure, a value of the activation energy for diffusion in the product layer was determined as 104 kJ/mol, a value which is in accordance with results (120 kJ/mol) published by De Hemptinne, (1990).

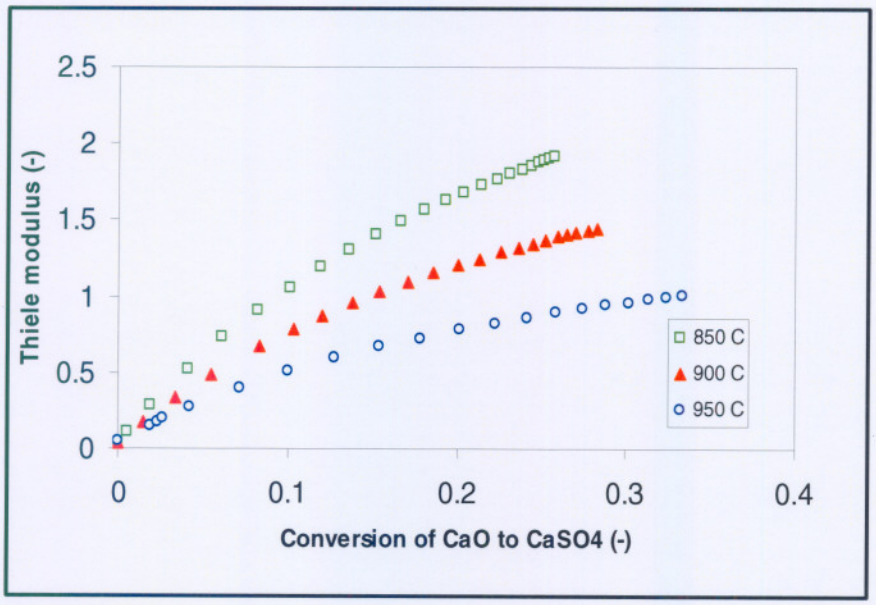

Figure 5.15: Thiele modulus as a function of conversion and temperature for dolomite A

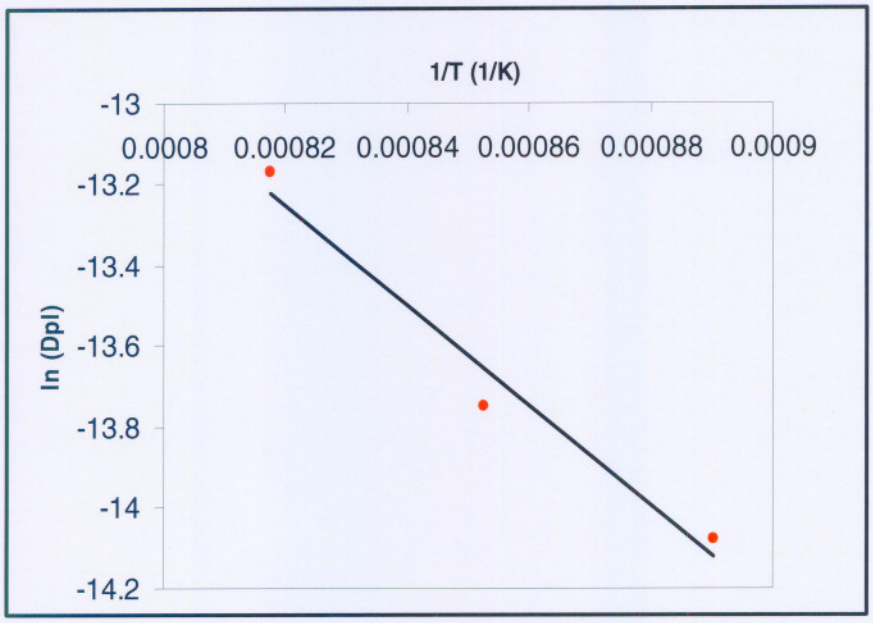

Figure 5.16: Arrhenius plot for the diffusivity in the product layer for Dolomite A

The comparison of experimental results and USC - VED model for Dolomite B is given in Figure 5.17. From this figure, it could be seen that the model does not fit the experiments at 850 and 900°C, but predicts the experiments at 950°C adequately. The disagreement between the experimental and model results for results obtained at 850 and 900°C can be attributed to the presence of magnesium oxide in the product layer which affects the effective diffusivity according to a different (temperature dependant) mechanism than that applicable at the highest temperature of 950°C. This needs to be examined further with more samples with different magnesium oxide concentrations. The fitted values at 950°C were compared to dolomite A and are given in Table 5.6. It can be seen from this table that the diffusion coefficient in the product layer of dolomite B is larger than that of dolomite A, which explains that faster conversion rate of B compared to A.

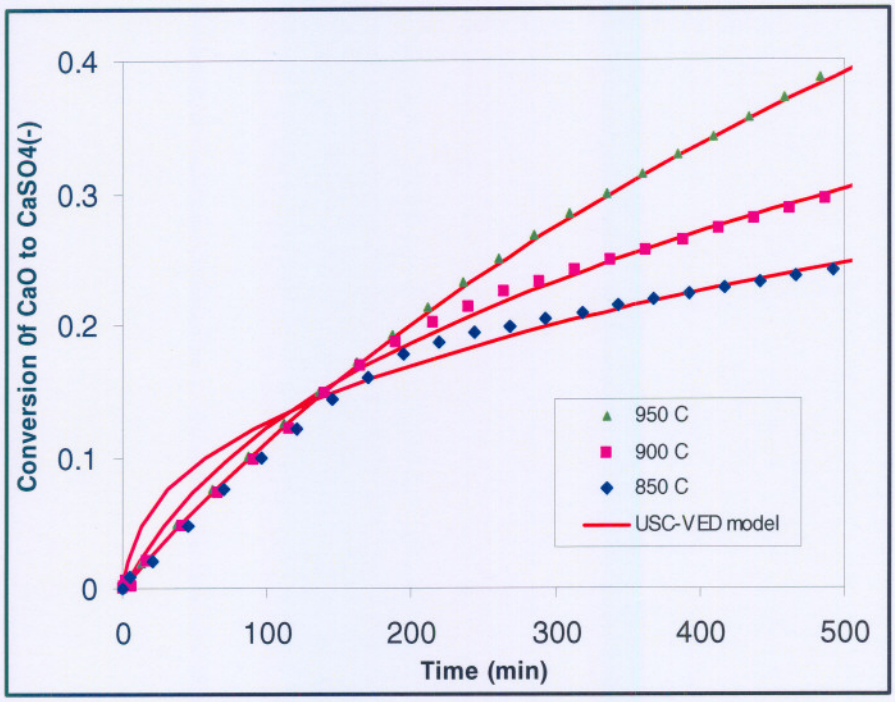

Figure 5.17: Dolomite B: Comparison of experimental results with calculated results (USC – VED) model

Table 5.6: Comparison of fitted and calculated parameters of dolomite A and B at 950°C.

	Dolomite A	Dolomite B
τ_R (min)	2310	2439
B (-)	140	78
k_s (10^{-2} m/min)	5.50	3.48
D_{pl} (10^{-7} m²/min)	19.1	28.9

5.4.4.2 Comparison with the unreacted shrinking core model

If the experimental results are fitted according to the USC - model, the final results, as given in Figure 5.18, are obtained. The USC - model also describes the experimental

results adequately, but a worse fit compared to the USC - VED is obtained. If the sum of the squared differences between experiments and model of the USC and USC - VED are compared, it is obtained that the deviation of the USC - VED is 29% (850°C) – 44% (950°C) less than the USC - model, indicating that the USC - VED is indeed a refinement to the USC model. Moreover, the USC - VED accounts for the change in resistance from kinetic to a combination of kinetic and diffusion, as was given in Figure 5.16, making it a preferred model above the USC model.

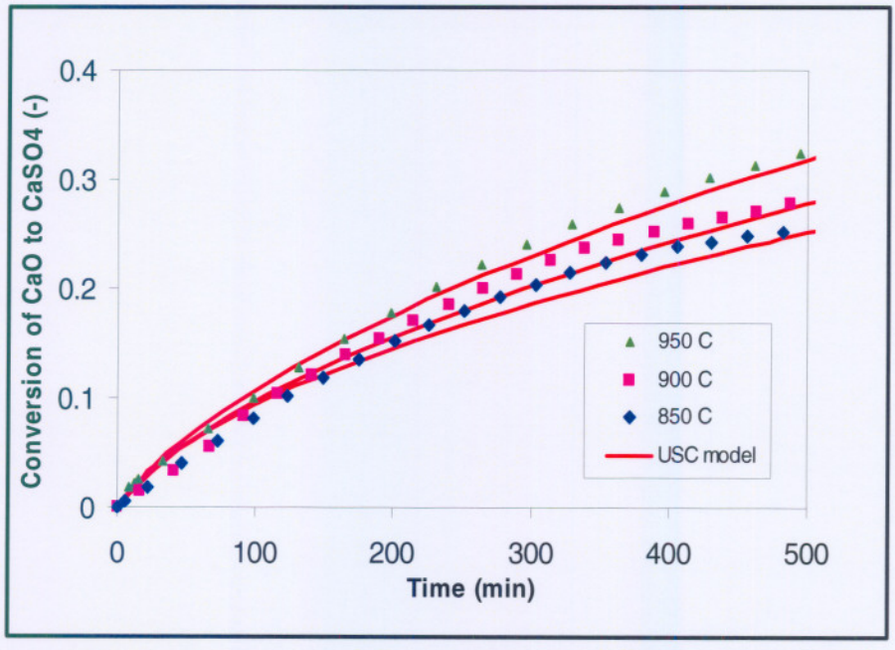

Figure: 5.18: Dolomite A: Comparison of experimental results with calculated results (USC) model.

CHAPTER 6
CONCLUSIONS AND RECOMMENDATIONS

6.1 Conclusions

The conclusions are the following:

1. The characterization analysis of the two dolomites supplied showed that:
   - the major difference between the samples was the calcium and magnesium compositions.
   - the pore size distributions were non - uniform consisting of micro-, meso- and macro pores with total porosities (mercury porosimetry) of the order of 0.23 and 0.28 respectively, which is not unusual for naturally occurring dolomites.
   - thermal cracking (detected on surface) occurred during the calcination and adsorption of the dolomite samples, which can lead to fragmentation in a fluidized bed.

2. Recarbonation of CaO was found to occur at temperatures and carbon dioxide partial pressures different to the theoretical phase equilibrium values which can be attribute to the different calcium solid phases (solution) present in the dolomites. For gas mixtures with a concentration of 8% (mole) CO_2 and above 850°C it was established that no recarbonation occurred while at 800°C there was a phase transition which is different to the theoretical predictions using pure compounds. With high concentrations of carbon dioxide (25%) and at a high temperature (950°C) far from the transition point some physical adsorption or reaction of carbon dioxide with the dolomites were detected which needs to be confirmed by another investigation.

3. From an analysis consisting of comparing results involving recarbonation (CO_2/N_2) with simultaneous recarbonation and sulphation ($SO_2/CO_2/O_2/N_2$) it was confirmed that the recarbonation reaction rate is very fast with respect to the sulphation rate of either $CaCO_3$ or CaO and that in the simultaneous case the sulphation of CaO does not occur because of the rapid conversion to $CaCO_3$

which in turn is sulphated. This case would not however arise in practice since sulphation with $CaCO_3$ would involve starting with the raw dolomite, which would consist of essentially of $CaCO_3$ (no calcination).

4. The sulphation results involving the conversion of CaO to $CaSO_4$ over very long periods of time (500 minutes) showed that there is no blocking - off of pores. Conversion results are ever increasing over this period of time with a decreasing rate, whereas results published show practically zero rates after periods as low as 10 minutes.

5. The adsorption capacity (conversion of CaO) for the two dolomites was found to be slightly different with the dolomite consisting of more magnesium being consistently more active. After 500 minutes the conversion levels for the two dolomites vary over a range of between 23% and nearly 40% at 850 to 950°C. When compared with published results at a reference time of 120 minutes, conversion levels obtained in this study of the order of 10% to 15%, are similar to results reported for some limestones by a number of investigators. There are however results reported involving both limestones and dolomites which are much more effective. Unfortunately, a meaningful comparison with published results could not be achieved because of a lack of information concerning the structures of the dolomites examined.

6. The unreacted shrinking core model with variable effective diffusivity is a refinement on the unreacted shrinking core model and can successfully describe the conversion of CaO to $CaSO_4$ for the dolomite with a low magnesium content. It was shown that this conversion is accomplished with a transition from reaction controlled to a combination of reaction and diffusion controlled during conversion. This phenomenon cannot be modelled using the unreacted shrinking core model, and therefore a better fit with the unreacted shrinking core model with variable effective diffusivity was obtained. The dolomite sample with a higher concentration of magnesium showed a faster conversion rate and the conversion could only be described satisfactory according to the unreacted shrinking core with variable effective diffusivity at 950°C.

7. The results obtained in this investigation are applicable to desuphurization (SO_2) in atmospheric pressure fluidized bed combustors at temperatures above 850°C and with a low partial pressure of carbon dioxide of the order of 8% (mole), involving the sulphation of calcium oxide produced by calcination of raw dolomites. For FBC at temperatures below 800°C the sulphation reaction with calcium carbonate is the determining reaction, which needs to be investigated in detail for the respective dolomites.

6.2 Recommendations

This investigation was confined to desuphurization at atmospheric pressure with two dolomites and it is recommended that the following be investigated in order to expand on the results obtained.

1. More limestones and dolomites samples be examined to determine the effect of the presence of magnesium oxide.
2. More accurate structural analysis be done to assess the full spectrum of pore properties, which can be incorporated in more realistic models such as the random pore model.
3. Measurement of the different minerals present in the limestones and dolomites be done and that phase equilibria be measured experimentally and confirmed with theoretical results (advanced computer package).
4. That the physical adsorption properties of the adsorbents be assessed involving essentially carbon dioxide in order to explain results obtained.
5. That an investigation involving sulphation at low temperatures with low concentrations of carbon dioxide (with $CaCO_3$) be carried out with raw adsorbents and compared with results obtained in this investigation.
6. That more realistic reaction rate model be developed to account for diffusion throughout the whole adsorbent particle, such as the random pore model with modifications.
7. That the results obtained be evaluated against pilot plant results generated at Eskom.

REFERENCES

ADANEZ, J., LABIANO, F. G., ABANADES, J. C. and DIEGO, L. F. 2004. Direct sulfidation of half calcined dolomite under pressurized conditions, Industrial Engineering Chemistry and Research, 43: 4132 – 4139.

ALLEN, T. 1990. Particle size measurement, 4th edition E.I Dupont de Nemour and Company, Wilmington, Delaware.

ALVAREZ, E. and GONZALEZ, J.F. 1999. High - pressure thermo gravimetric analysis of the direct sulphation of Spanish calcium – based sorbents, Fuel, 78: 341 – 348.

AMAND, L. E., JOHANSSON, S., KARLSSON, M., LECKNER, B. 1986. Emissions from a fluidized bed boiler, Report A86 – 156, Department of Energy Conversion, Chalmers University of Technology, Gothenburg, Sweden.

BHATIA, S.K. and PERLMUTTER, D.D. 1980. A random pore model for fluid – solid reactions. Isothermal, Kinetic control, AICHE Journal, 26: 379 – 385.

BORGWARDT, H. R. 1970. Kinetics of the reaction of SO_2 with calcined limestone, Environmental Science and Technology, 4: 59 – 63.

BORGWARDT, H. R., ROCHE, N.F., and BRUCE, K.R. 1986. Method for variation of grain size in studies of gas - solid reactions involving CaO, Industrial and Engineering Chemistry Fundamentals, 25: 165 – 169.

BORGWARDT, H. R., BRUCE, K.R. and BLAKE, J. 1987. Investigation of product layer diffusivity for CaO sulfation, Industrial Engineering Chemistry and Research, 26: 1993 – 1998.

CARBERRY, J. J. 1976. Chemical and catalytic reaction engineering, McGraw Hill, New York.

CHEN , Z., Lin, M., IGNOWSKI, J., KELLY, B., LINJEWILE, T.M. and ARGAWAL, P.K. 2001. Mathematical modeling of fluidized bed combustion, Fuel, 80: 1259 – 1272.

CHIUNG, F.L., SHIH – MIN, S. and REN – BIN L. 2004. Kinetic model for the reaction of $Ca(OH)_2$/Fly ash sorbents with SO_2 at low temperatures, Industrial Engineering Chemistry and Research, 43: 4112 – 4117.

CIGDEM, G., GULSEN D. and TIMUR D. 2001. Kinetics of trona sulphur dioxide reaction, Chemical Engineering Science, 40: 13 - 18.

DAM - JOHANSEN, K. and OSTERGAARD, K. 1991. High temperature reactions between sulphur dioxide and limestone I. Comparison of limestones in two laboratory reactors and a pilot plant, Chemical Engineering Science, 46: 827 – 837.

DAM - JOHANSEN, K., HANSEN, P.F.B. and OSTERGAARD, K. 1991. High - temperature reaction between sulphur dioxide and limestone III. A grain - model – micrograin model and its verification, Chemical Engineering Science, 46: 847 – 853.

De HEMPTINNE, J.C. 1990. Sulfation of nonporous calcium oxide, PhD Thesis, Massachusetts Institute of Technology, Department of Chemical Engineering, Cambridge, USA.

Do, D.D., 1998. Adsorption analysis: Equilibria and Kinetics, University of Queensland, Australia. ISBN 1 - 86094 -130 – 3.

ESKOM, 2003. Generation Communication. http://www.eskom.co.za

EVERSON, R.C., NEOMAGUS, H.W.J.P. and NGELEKA, T.P. Sulphur dioxide capture under low pressure fluidized bed combustion conditions, Indaba 2005: Eleventh Southern African conference on coal science and technology, Fossil Fuel Foundation of Africa, November 2005.

FERNANDEZ, M.J. and LYNGFELT A. 2001. Concentration of sulphur compounds in the combustion chamber of a circulating fluidized bed boiler, Fuel, 80: 321-326

FERNOULI, L.A. and LYNN, S. 1995. Study of calcium based sorbents for high temperature H_2S removal.1. Kinetics of H_2S sorption by uncalcined limestone, Industrial Engineering Chemistry and Research, 34: 2324 – 2333.

FUERTES, A.B., VELASCO, G., ALVAREZ, T. and FERNANDEZ, M.J. 1995. Sulfation of dolomite particles at high CO_2 partial pressures, Thermochimica Acta, 254: 63 – 78.

FULLER, N. E., SCHETTLER, D. P. and GIDDINGS, J. C. 1966. A new method for prediction of binary gas - phase diffusion coefficients, Industrial Engineering Chemistry, 58: 19 – 27.

GARCIA, F., ABAD, A., de DIEGO, P.and ADANEZ, J. 2002. Calcination of calcium based sorbents at pressure in a broad range of CO_2 concentrations, Chemical Engineering Science, 57: 2381 – 2393.

GHARDASHKHANI, G. and COOPER, D.A., 1990. A thermo gravimetric study of the reaction between sulphur and calcium oxide, Thermochimica Acta, 161: 327 - 337.

GREGG, S.J. and SING, K.S.W. 1982. Adsorption, surface area and porosity, Academic Press, Inc., London, New York.

HAO, L. and BERNARD, M.G. 1998. The influence of limestone addition at different positions on gaseous emissions from coal fired circulating fluidized bed combustor, Fuel, 77: 1569 – 1577.

HARTMAN, M. and COUGHLIN, R.W. 1976. Reaction of sulphur dioxide with limestone and the grain model, AICHE Journal, 22: 490 – 498.

IISA, K. 1992. Sulphur capture under pressurized fluidized bed combustion conditions, Doctoral Thesis. Abo Akademi, Turka, Finland.

IISA, K., TULLIN, C. and HUPA, M. 1991. Simultaneous sulphation and recarbonation of calcined limestone under PFBC conditions. International Conference on Fluidised Bed Combustion, Editor: E.J. Anthony Canmet, Book No. 10312A - 1991, 83 - 90.

IISA, K.P. and HUPA, M. 1990. Sulphur adsorption by limestone at pressurized Fluidised Bed Conditions, Twenty-third Symposium (International) on Combustion, 943 - 948.

IRFAN, A. and BALCI, S. 2002. Sulphation reaction between SO_2 and limestone, Fuel, 41: 179 -188.

LINDNER, B. and SIMONSSON, D. 1981. Comparison of structural models for gas - solid reactions undergoing structural changes, Chemical Engineering Science, 36: 1519.

LYNGFELT, A. and LECKNER, B. 1999. Sulphur capture in circulating fluidized bed boilers: Can the efficiency be predicted? Chemical Engineering Science, 54: 5573 – 5584.

MAHESH, V.I., HIMANSHU, G., BARTEV, B. and Fan, L.S. 2004. Multicyclic study on the simultaneous carbonation and sulfation of high – reactivity CaO, Industrial Engineering Chemistry and Research, 43: 3939 – 3947.

MATTISSON, T. and LYNGFELT, A. 1998. A sulphur capture model for circulating fluidized bed boilers. Chemical Engineering Science, 53: 1163 –1173

NEOMAGUS, H.W.J.P., SARACCO, G., WESSEL, H.F.W. and VERSTEEG, G.F. 2000. The catalytic combustion of natural gas in a membrane reactor with separate feed of reactants, Chemical Engineering Journal, 77, 165 177.

NIMMO, W. PASTIAS, A. A., HAMPARTSOUMIAN, E., GIBBS, B. M. and WILLIAMS P. T. 2004. Simultaneous reduction of NOx and SO_2 emissions from coal combustion by calcium magnesium acetate, Fuel, 83: 149 – 155.

NOWAK, W. and MUSKALA, W. 2001. Clean and ecological coal combustion in the binary circulating fluidized bed, Energy, 26: 1109 – 1120.

O'Neill, E.P., KEAIRNS, D. L. and KITTLE, W.E. 1976. The thermo gravimetric study of the sulphation of limestone and dolomite. The effect of calcination conditions, Themochimica Acta, 14: 209 - 220.

OZER, A.K., GULABOGLU, M.S., BAYRAKCEKEN, S. and WEISWEILER, W. 2002. Flue gas desulfurization with phosphate rock in a fluidized bed, Fuel, 81: 41 – 49.

PARTANEN, J. 2004. Chemistry of HCL and limestone in Fluidized bed Combustion. PhD Thesis: Abo Akademi, Faculty of Chemical Engineering.

SIMONS, G.A. and GARMAN, A.R. 1986. Small pore closure and the deactivation of the limestone sulfation reaction, AICHE Journal, 32, 1491 – 1499.

STANELY - WOOD, N.G. and LINES, R.W. 1992. Particle Size Analysis, Royal Society of Chemistry, University of Technology, Loughborough, UK.

STENCEL, M.J., YANG J. and NEARTHER, J.K. 1995. Desulphurization of bituminous coals: Fluidized bed gasification of coal /phosphoric acid mixtures, Fuel Processing Technology, 41: 135 -146.

SMITH, J.M., VAN NESS, H.C. and ABBOTT M.M. 1996. Introduction to Chemical Engineering Thermodynamics, McGraw – Hill, New York.

TADAAKI, S., MIRKO, P., KAZUAKI, Y., MASATO, T. S. S. 2002. A simplified model of SO_2 capture by limestone in 71 MWe pressurized fluidized bed combustor Chemical Engineering Science, 57: 4117 – 4128.

TOPPER, J. M., CROSS, P. J. I. and GOLDTHORPE, S. H., 1994. Clean coal technology for power and cogeneration, Fuel, 73: 1056 – 1063.

TRIKKEL, A. and KUUSIK, R. 2003. Modeling of decomposition and sulphation of oil shale carbonates on the basis of natural limestone, Estonian Academy Publishers, 20: 491 - 500.

TSUTOMU, N., YAN – BAI, L., MASAYUKI, K., NOBUYOSHI, N. and KUNIO, K. 2003. H_2S removal by fine limestone particles in a powder – particle fluidized bed, Industrial Engineering Chemistry and Research, 42: 3413 – 3419.

TULLIN, C. and LJUNGSTROM, E. 1989. Reaction between calcium carbonate and sulphur dioxide, Energy and Fuels, 3: 284 - 287.

ULERICH, N.H., NEWBY, R.A. and KEAIRNS, D.L. 1980. A thermo gravimetric study of the sulfation of limestone and dolomite – prediction of pressurized and atmospheric fluidized bed desulfurization, Thermochimica Acta, 36: 1 – 16.

VAN DER RIET, M. 2005. Eskom, Private Communication.

WANG, C., SHEN, X. and Xu, Y. 2002. Investigation on sulphation of modified Ca – based sorbent, Fuel Processing Technology, 79:121 – 133.

WASI, Z. K. and BERNARD, M.G. 1995. The influence of staging in the reduction of SO_2 by limestone in the fluidized bed combustor, Fuel, 74: 800 – 805.

YONG, Z. and RODRIGUES, A.E. 2002. Adsorption of carbon dioxide at high temperature: a review. Separation and Purification Technology, 26: 195 - 205.

YRJAS, P., IISA, K. and HUPA, M. 1995. Comparison of SO_2 capture capacities of limestone and dolomite under pressure, Fuel, 74: 395 - 400.

ZEVENHOVEN, C.A.P., YRJAS, K. P. and HUPA, M. 1996. Hydrogen sulphide capture by limestone and dolomite at elevated pressure. 2. Sorbent particle conversion modelling, Industrial Engineering Chemistry and Research, 35: 943 - 949.

ZEVENHOVEN, A.P.C., YRJAS, K.P. and HUPA, M. 1998a. Product layer development during sulfation and sulfidation of uncalcined limestone particles at elevated pressures, Industrial Engineering and Chemistry Research, 37: 2639 - 2646.

ZEVENHOVEN, R., YRJAS, K. P. and HUPA, M. 1998b. Sulphur dioxide capture under PFBC conditions: the influence of sorbent particle structure, Fuel, 77: 285 - 292.

ZHANG, L., SATO, A., NINOMIYA, Y. and SASAOKA, E. 2003. In situ desulphurization during combustion of high – sulfur coal added with sulfur capture sorbents, Fuel, 82: 255 – 266.

ZHANGFA, W., 2003. Clean fuels from coal, IEA Clean Coal Center, United Kingdom

APPENDIX A: Thermodynamic equilibrium calculations

A.1 Calcium oxide - calcium carbonate - carbon dioxide equilibria

The chemical equation is

$$CaCO_{3(s)} = CaO_{(s)} + CO_{2(g)}$$

The following equations are applicable (Smith et al., 1996)

The partial pressure of CO_2

$$p_{CO_2} = K \tag{A.1}$$

The equilibrium constant

$$\mathrm{K} = \exp\frac{-\Delta G^o}{RT} \tag{A.2}$$

The change in Gibbs Free Energy

$$\frac{\Delta G^o}{RT} = \frac{\Delta G_0^O - \Delta H_0^O}{RT_0} + \frac{\Delta H_0^O}{RT} + \frac{1}{T}\int_{T_0}^{T}\frac{\Delta Cp}{R}dT - \int_{T_0}^{T}\frac{\Delta Cp}{R}\frac{dT}{T} \tag{A.3}$$

with temperature dependant heat capacities

$$C_p = A + BT + CT^2 + DT^{-2} \tag{A.4}$$

the following is obtained

$$\int_{T_0}^{T}\frac{\Delta C_P}{R}dT = \mathrm{A}\Delta T_0(\tau_0 - 1) + \frac{\Delta \mathrm{B}}{2}T_0^2(\tau_0{}^2 - 1) + \frac{\Delta C}{3}T_0^3(\tau_0{}^3 - 1) + \frac{\Delta D}{T_0}\left(\frac{\tau_0 - 1}{\tau_0}\right) \tag{A.5}$$

$$\int_{T_0}^{T} \frac{\Delta C_P^o}{R}\frac{dT}{T} = \Delta A \ln \tau_0 + \left[\Delta B T_0 + \left(\Delta C T_0^2 + \frac{\Delta D}{\tau_0^{\,2} T_0^2}\right)\left(\frac{\tau_0 + 1}{2}\right)\right](\tau_0 - 1) \qquad \text{(A.6)}$$

with $\tau_0 = \dfrac{T}{T_o}$

With these equations and data available from Smith *et al.*, (1996) the results shown in Table A.1 were obtained:

Table A.1: Equilibrium constants and partial pressures for $CaO\text{-}CaCO_3\text{-}CO_2$

T (K)	T (^{0}C)	K	p_{CO_2} (bar)
298	25	1.39×10^{-23}	1.39×10^{-23}
623	350	2.35×10^{-7}	2.39×10^{-7}
823	550	8.39×10^{-4}	8.39×10^{-4}
923	650	1.27×10^{-2}	1.27×10^{-2}
1023	750	1.12×10^{-1}	1.12×10^{-1}
1123	850	6.59×10^{-1}	6.59×10^{-1}
1223	950	2.8	2.8
1323	1050	9.56	9.56
1423	1150	27.1	27.1

A.2: Magnesium oxide - magnesium carbonate - carbon dioxide equilibria

The chemical equation is

$$MgCO_3 = MgO + CO_2$$

The equation derived by Fuertes *et al.*, (1995) was used and results are shown in Table A.2

$$p_{CO_2}/(bar) = 1.339 \times 10^9 e^{-14145/\,T(K)} \qquad \text{(A. 7)}$$

Table A.2: Equilibrium constants and partial pressures for $MgO\text{-}MgCO_3\text{-}CO_2$

T (K)	T (°C)	K	p_{CO_2} (bar)
523	250	2.36×10^{-3}	2.36×10^{-3}
623	350	1.82×10^{-1}	1.82×10^{-1}
723	450	4.21	4.21
823	550	4.55×10^{1}	4.55×10^{1}
923	650	2.93×10^{2}	2.93×10^{2}
1023	750	1.31×10^{3}	1.31×10^{3}
1123	850	4.50×10^{3}	4.50×10^{3}
1223	950	1.26×10^{4}	1.26×10^{4}
1323	1050	3.02×10^{4}	3.02×10^{4}

APPENDIX B: Results of sulphation experiments

B.1 Introduction

Results from the sulphation experiments for both dolomite A and dolomite B are presented. Experiments were conducted at different temperatures and CO_2 partial pressures. Experiments, with the gas atmosphere of 2500 ppm SO_2, 6.8 % O_2, 14 % CO_2 and balance N_2 and those of 25 % CO_2 with 4 % O_2 were conducted at 750 and 950°C. Those experiments with 8 % CO_2 partial pressure were conducted over the range 850 to 950°C with a 50°C difference.

B.2 Dolomite A results with 2500 ppm SO_2, 8% CO_2, 6.8 % O_2 and balance N_2.

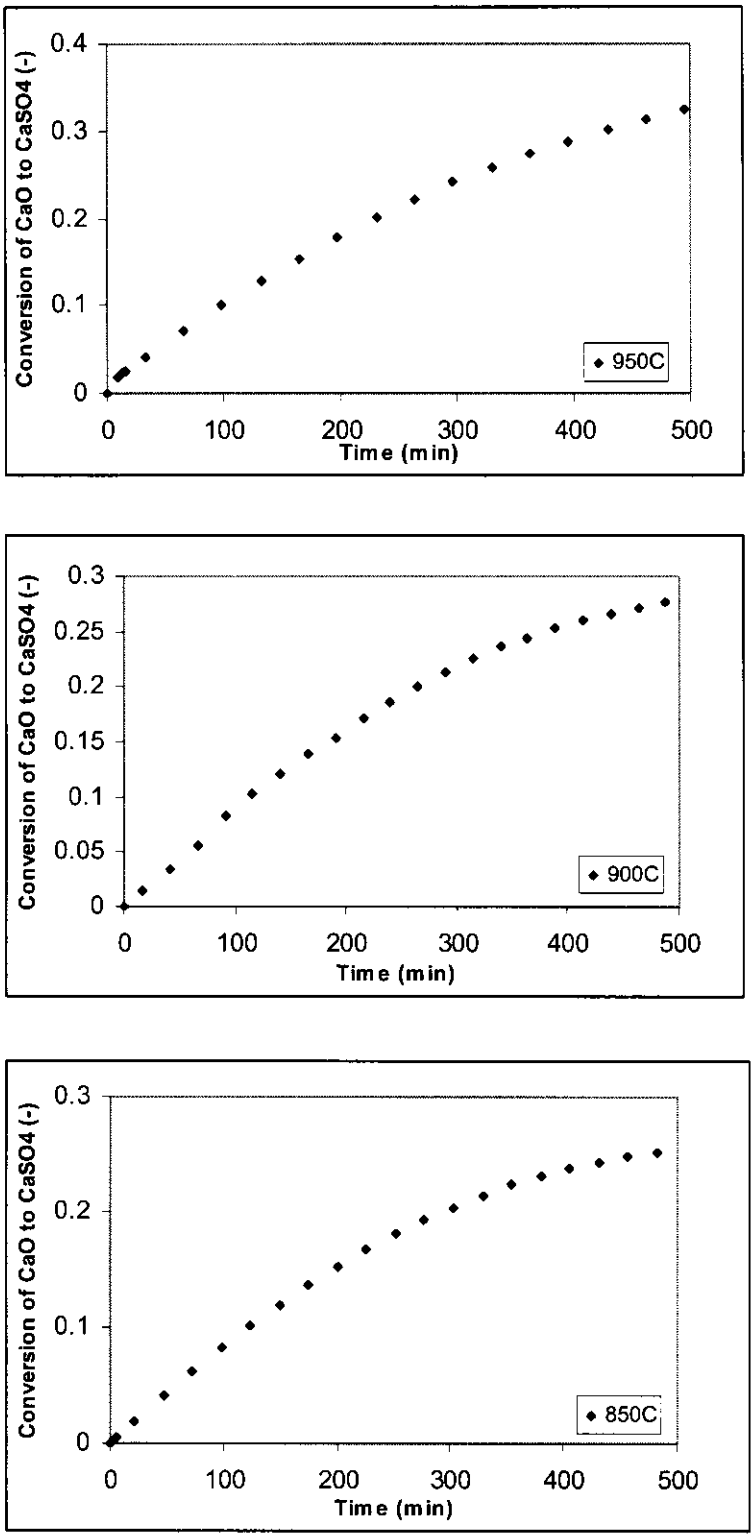

Figure B.1: Dolomite A results with 8% CO_2

B.3 Dolomite B results with 2500 ppm SO_2, 8% CO_2, 6.8 % O_2 and balance N_2.

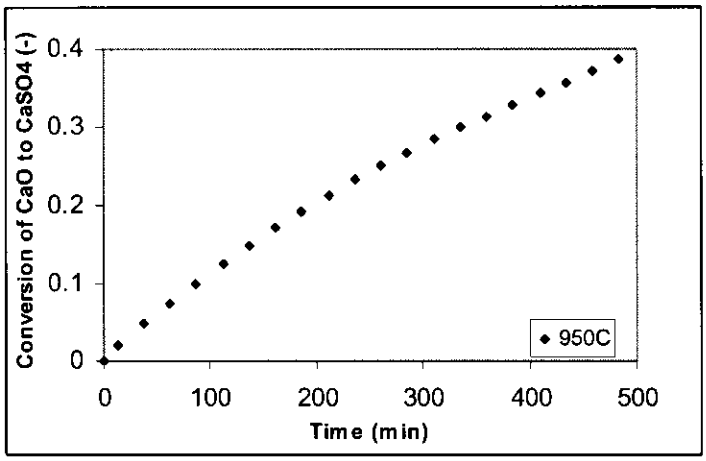

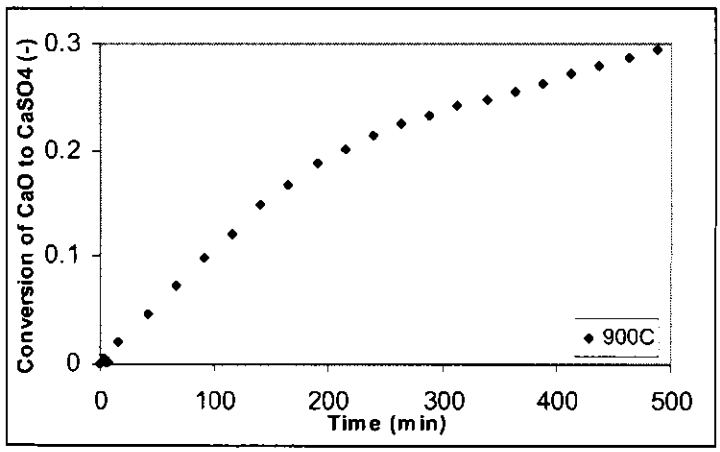

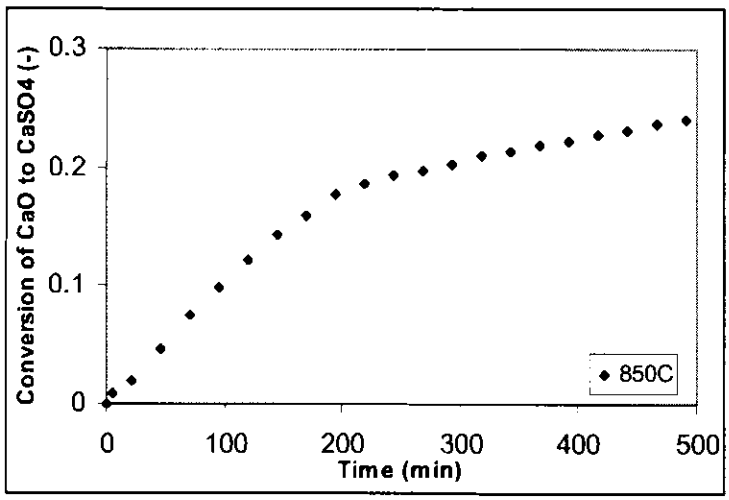

Figure B.2: Dolomite B results with 8% CO_2

B.4 Dolomite A results with 2500 ppm SO_2, 14% CO_2, 6.8 % O_2 and balance N_2.

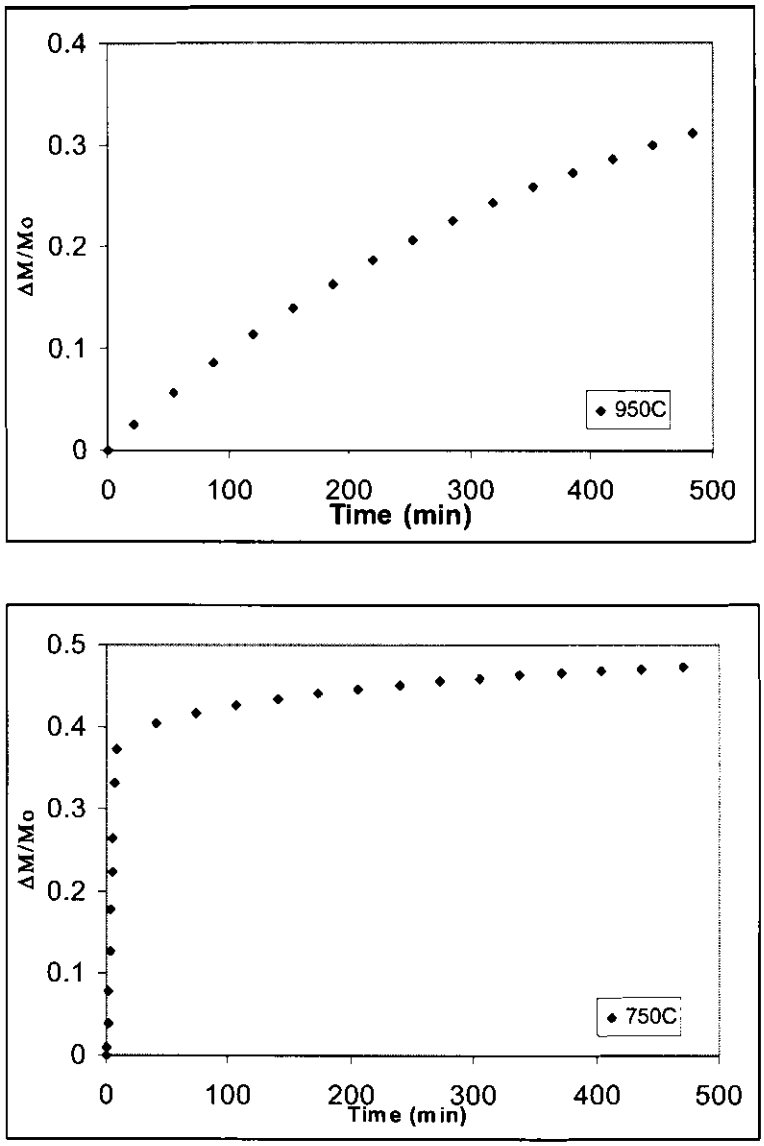

Figure B.3: Dolomite A results with 14% CO_2

B.5 Dolomite B results with 2500 ppm SO_2, 14% CO_2, 6.8 % O_2 and balance N_2.

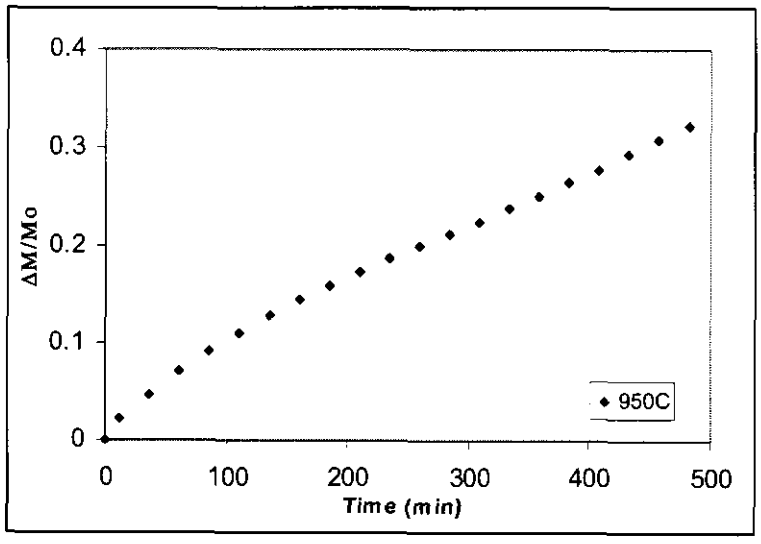

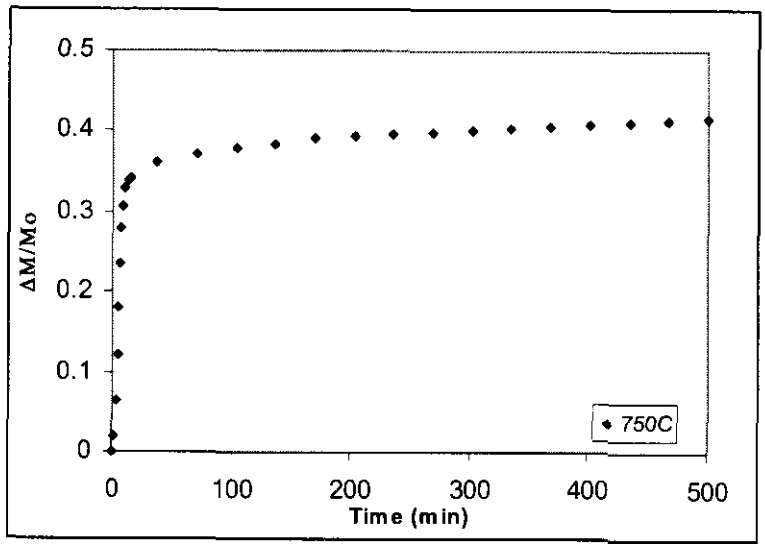

Figure B.4: Dolomite B results with 14% CO_2

B.6 Dolomite A results with 2500 ppm SO_2, 25% CO_2, 4 % O_2 and balance N_2.

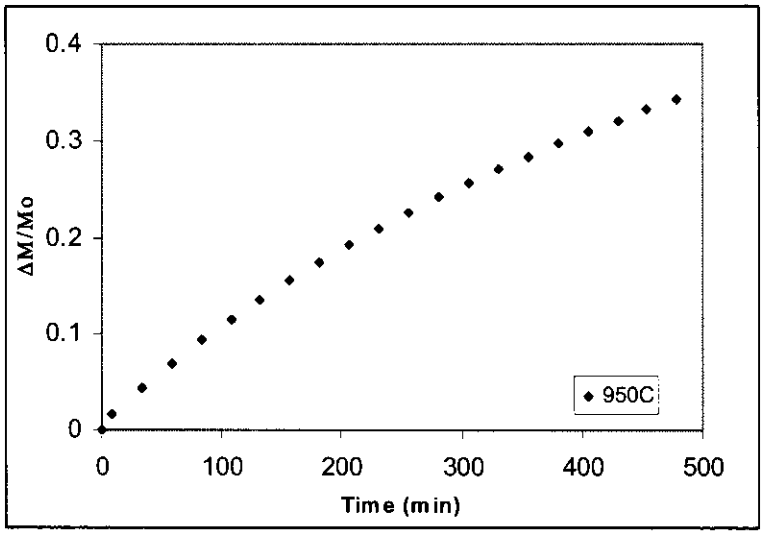

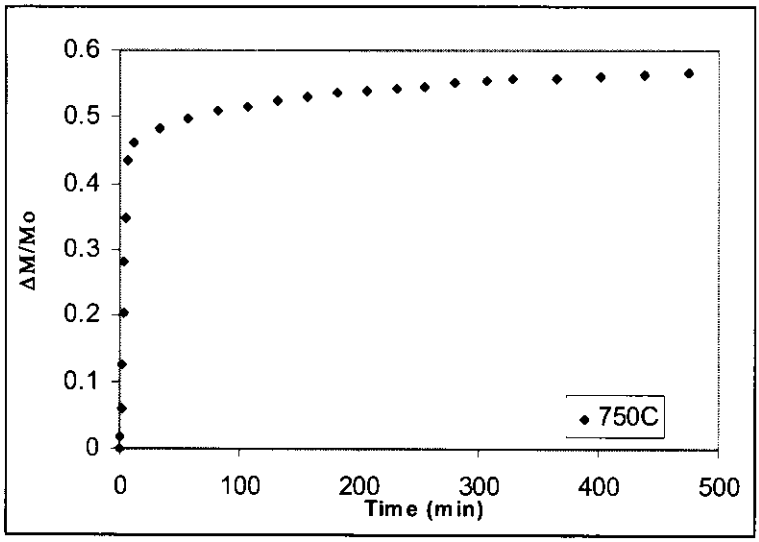

Figure B.5: Dolomite A results with 25% CO_2

B.6 Dolomite B results with 2500 ppm SO_2, 25% CO_2, 4 % O_2 and balance N_2.

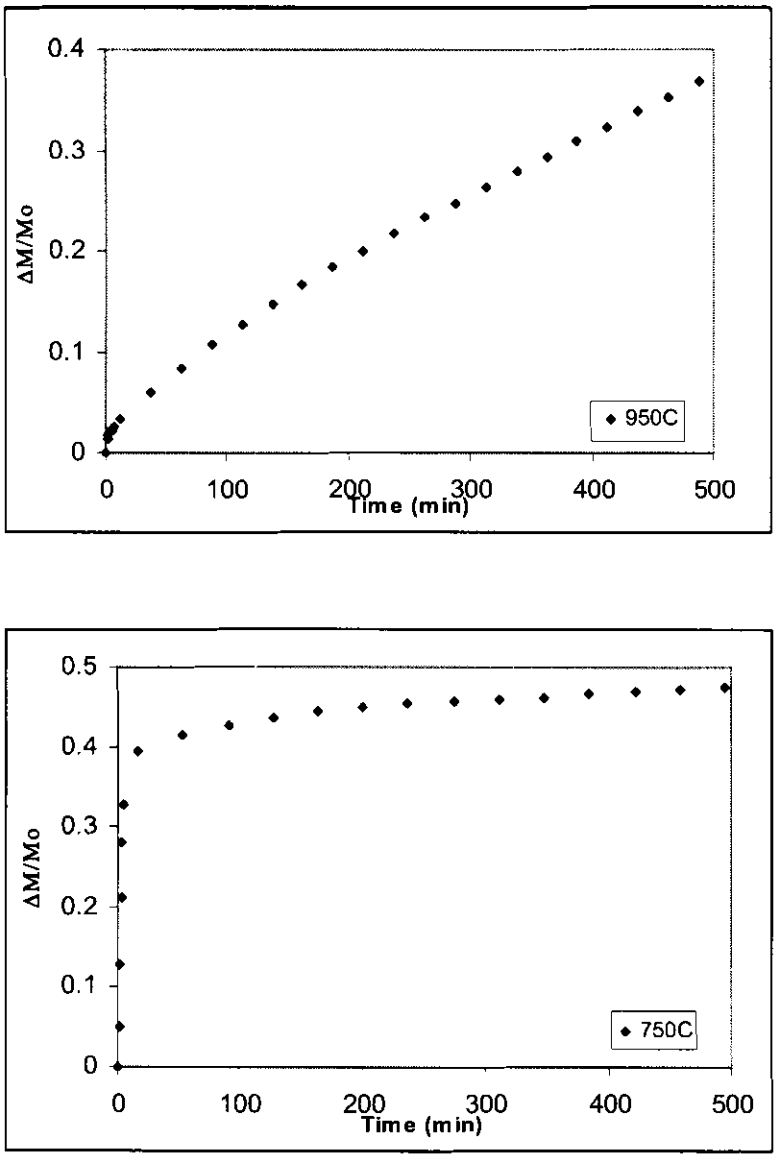

Figure B.6: Dolomite B results with 25% CO_2